Energy Efficient Buffer-Aided Transmission Scheme in Wireless Powered Cooperative NOMA Relay Network

Xiaolong Lan, Yongmin Zhang, *Member, IEEE*, Qingchun Chen, *Senior Member, IEEE*, and Lin Cai, *Fellow, IEEE*

***Abstract*— In this paper, we consider a wireless powered cooperative non-orthogonal multiple access (NOMA) relay network, in which one source is supposed to send independent messages to two users with the assistance of one energy-constrained relay that harvests energy from the source. Firstly, we study the minimum power consumption at the source node to fulfill the least required transmission rates by two users in both time switching relaying (TSR) strategy and power splitting relaying (PSR) one. Secondly, when the relay is provisioned with data buffer and energy storage, the long-term average power consumption minimization problem is formulated to take into account of the data and energy queue causality, peak transmit power constraint, and transmission mode selection. By using Lyapunov optimization framework, a novel buffer-aided transmission scheme (BATS) is proposed to asymptotically approach the optimal solution. Our analysis shows that, the PSR outperforms the TSR in terms of the realized energy efficiency, and BATS can be utilized to further improve the energy efficiency. It is disclosed that, there is an inherent trade-off between the long-term power consumption and the average queuing delay. In addition, larger user rates or less power consumption can be realized if a larger delay can be tolerated.**

***Index Terms*— Buffer-aided transmission, cooperative NOMA relay network, energy efficiency.**

I. Introduction

NON-ORTHOGONAL multiple access (NOMA) technique provides us a promising solution to improve spectral efficiency and to support massive connectivity in mobile communication network. Recently it has attracted considerable attentions in the society [1]–[6]. Unlike the conventional orthogonal multiple access techniques (OMA), NOMA allows multiple users to be served simultaneously at different power levels in the same resource blocks, either in time, frequency, or code domain. By using the superposition code at the transmitter and successive interference cancellation (SIC) at the receivers, the user with the best channel condition can successfully detect and eliminate the co-channel interference from those users with inferior channel qualities. When compared with the OMA techniques, the NOMA ones can effectively improve the utilization of scarce resources.

Meanwhile, simultaneous wireless information and power transfer (SWIPT) technique provides a promising solution to prolong the lifetime of energy-constrained networks like the Internet-of-Things (IoTs) and wireless sensor networks (WSNs) [7]–[14]. SWIPT allows the energy-constrained node to extract both information and energy from the received radio frequency (RF) signals simultaneously. Time switching (TS) and power splitting (PS) based receiver architectures were proposed in [8], [9] to realize the SWIPT. In the TS based receiver, each time slot will be further sub-divided into two sub-slots, one for energy harvesting and one for information transmission. The PS based receiver allows the receiver to decompose the received RF signal into two streams for energy harvesting and information processing, respectively. Motivated by the benefits of NOMA and SWIPT, the new paradigm was introduced in [6], [11]–[14] by combining NOMA and SWIPT in order to prolong the lifetime of the energy-constrained networks and to support massive connectivity.

In addition, the buffer-aided relaying system has attracted much research attention since it opens up a new degree of freedom to improve the system capacity and energy efficiency [20], [21], [29]–[33]. For the buffer-aided relaying system, the relay can adaptively select operation mode between the relay reception and the relay transmission based on the current channel state information (CSI), which has been shown to be able to give rise to a larger network throughput at the cost of some increase in the queueing delay. Nonetheless, to the best of the authors' knowledge, there is few research effort to explore the impact of buffer-aided mechanism on the realized energy efficiency in the wireless powered cooperative NOMA networks, which motivates our work in this paper.

Manuscript received July 5, 2019; revised October 26, 2019 and December 3, 2019; accepted December 4, 2019. Date of publication December 13, 2019; date of current version March 18, 2020. This work was supported in part by the National Natural Science Foundation of China (NSFC) under Grant 61771406 and Grant 61702450, in part by the Chinese Scholarship Council (CSC), in part by the Natural Sciences and Engineering Research Council of Canada (NSERC), and in part by the Compute Canada. The associate editor coordinating the review of this article and approving it for publication was R. C. De Lamare. *(Corresponding author: Qingchun Chen.)*

X. Lan is with the Department of Electronics and Communication Engineering, Guangzhou University, Guangzhou 510006, China, and also with School of Information Science and Technology, Southwest Jiaotong University, Chengdu 611756, China (e-mail: xiaolonglan1112@gmail.com).

Y. Zhang is with the School of Computer Science, Central South University, Changsha 410083, China (e-mail: zhangyongmin@csu.edu.cn).

Q. Chen is with the Department of Electronics and Communication Engineering, Guangzhou University, Guangzhou 510006, China (e-mail: qcchen@gzhu.edu.cn).

L. Cai is with the Department of Electrical and Computer Engineering, University of Victoria, Victoria, BC V8W 3P6, Canada (e-mail: cai@ece.uvic.edu).

Color versions of one or more of the figures in this article are available online at http://ieeexplore.ieee.org.

Digital Object Identifier 10.1109/TCOMM.2019.2959336

In this paper, we consider the wireless powered cooperative NOMA relay network, in which one source is supposed to send independent messages to two users with the assistance of one half-duplex energy-constrained relay that harvests energy from the source. In addition, the NOMA scheme is assumed at the relay to forward data from the source to both users. To address the energy efficiency issue, we consider to minimize the power consumption at the source node when the system is supposed to fulfill the required transmission rates by two users with either the time switching based relaying (TSR) strategy or the power splitting based relaying (PSR) one. The relay is further assumed to be provisioned with data buffer and energy storage to store the received data and the harvested energy temporarily. Now the relay can adaptively switch its transmission mode amongst energy harvesting, relay receiving, and relay transmitting according to the current CSI, the energy consumption state information (ESI) and the data buffer state information (BSI). In this setup, the long-term average power consumption minimization problem is formulated to take into account of the data and energy queue causality, the peak transmit power constraint, and the transmission mode selection. To make the problem easier to be handled, we will show how to transform the long-term average power consumption minimization problem into a real-time optimization problem by using the Lyapunov optimization framework. On the basis, the buffer-aided adaptive transmission scheme (BATS) was derived. Our analysis results show that, the proposed BATS is capable of asymptotically approaching the optimal solution. The contributions of this paper can be briefly summarized as follows:

- When the relay is not provisioned with the data buffer, the minimal power consumption problem of both the PSR strategy and the TSR one are studied for the given required least data rates by two users. We derive the closed-form optimal solution for the PSR strategy. While for the TSR strategy, we show that the minimal power consumption can be determined through one-dimension line search. Numerical results are presented to show that, the PSR outperforms the TSR in terms of the realized energy efficiency performance.
- When the relay is provisioned with both data buffer and energy storage, the minimal power consumption problem was formulated for the given required least data rates by two users. And a novel BATS is developed to take into considerations of the rate allocation, power allocation, and transmission mode selection. Numerical results are presented to reveal that, when compared with the PSR and the TSR schemes, the proposed BATS can significantly improve the energy efficiency for the same required least data rates by two users.
- Our analysis discloses the inherent trade-off between long-term power consumption and the average queuing delay. It is shown that, less power consumption can be realized when the user can tolerate some increase in the transmission delay.

The remainder of this paper is organized as follows. Section II presents a related literature survey. The wireless powered cooperative NOMA relaying system model and the minimum power consumption analysis in both the PSR strategy and the TSR one are presented in Section III. The buffer-aided wireless powered cooperative NOMA relaying system model and the BATS scheme will be addressed in Section IV. Numerical analysis results are presented in Section V. Finally, we conclude our work in Section VI.

II. Related Work

As a promising technique to improve spectral efficiency, NOMA based relaying has recently attracted research attention. A cooperative NOMA with SWIPT was investigated in [6] to show that, the NOMA scheme could be utilized to significantly reduce the outage probability, when compared with the conventional OMA based SWIPT relaying networks. In the presence of imperfect CSIs, both the single-antenna relay and the multi-antenna relay were considered in [11] and [12] for the NOMA-based relaying networks. The relay selection issues were studied in [15]–[18] to improve transmission efficiency in the cooperative NOMA networks with multiple relays. A cooperative NOMA scheme with both direct link users and indirect link users was studied in [19] to reveal that, the cooperative NOMA scheme significantly outperforms the cooperative OMA one in terms of the realized coding gain without losing diversity order.

Meanwhile, the buffer-aided transmission scheme has attracted considerable attentions to improve transmission efficiency in recent years [20]–[33]. A novel link selection scheme was proposed for the buffer-aided relay network [20], in which the relay can adaptively decide whether to transmit or to receive data according to the involving CSI. It is shown that, when compared with the conventional relay protocols without buffering, the transmission efficiency can be significantly improved by using the buffer-aided relay protocol. In [21], a delay-aware adaptive transmission scheme was proposed for the buffer-aided two-way energy-constrained relay network to effectively improve the achievable rate region by deploying the data buffer and energy storage at the relay. In [22], the buffer-aided relaying scheme was proposed for the full-duplex relay network to maximize the long-term achievable rate, in which the relay can adaptively determine to either receive, transmit, or simultaneously receive and transmit. An opportunistic relaying protocol for the buffer-aided multi-relay network was proposed to minimize the total energy consumption for an inter-relay interference cancellation scheme in [23], and it is shown that, when relays are provisioned with data buffers, the energy efficiency and network throughput can be significantly improved. A buffer-aided multi-way relay selection scheme was studied in [24] to effectively exploit the best link in multi-way cooperative multi-antenna system. An adaptive buffer-aided distributed space-time coding scheme and a buffer-aided physical network coding technique was proposed for the wireless cooperative network in [25] and [26], respectively. It was shown that, with the help of buffers, the bit error rate can be significantly reduced because the buffer-aided mechanism provides the extra degree of freedom in choosing the best transmission channel. A novel buffer-aided relay

selection scheme was proposed for trust-aware relay networks in [27] to show that, a lower outage probability or a higher diversity order can be achieved with the help of buffer-aided mechanism. Moreover, by using infinite horizon partially observable Markov decision process, an energy-efficient optimal control problem was formulated for SWIPT-MIMO system in [28], and it is shown that, the antenna selection and beamforming power control scheme can be derived based on current data and energy queue state information to minimize the users' delay under the average power and transmission rate constraints. In addition, the transmission mode selection and power allocation were jointly optimized in [29] to maximize the long-term achievable rate region of the buffer-aided two-way relay network. Some novel link selection schemes for the buffer-aided multi-relay network were proposed to improve the network throughput [30], [32] and the outage probability [31].

Motivated by the great potential of buffer-aided transmission mechanism, some works had begun to investigate the buffer-aided NOMA network [36]–[41]. A joint user scheduling and power allocation scheme was proposed in [36] to minimize the long-term power consumption for the NOMA downlink networks. A joint user-and-hop scheduling scheme was proposed in [37] to maximize the long-term achievable rate region in the dual-hop system, in which two source-destination pairs share a buffer-aided relay. It was shown that, due to the advantages of buffer-aided mechanism, the multiuser and multihop diversity can be further exploited to improve the achievable rate region. The long-term network utility maximization problem was studied in [38] for the buffer-aided cooperative NOMA network, in which the working mode selection, admission control, and power allocation were jointly optimized. The outage probability of the buffer-aided NOMA relaying systems was analyzed in [39] in two scenarios of whether the relay knows the CSI or does not know the CSI. An adaptive transmission scheme was proposed to maximize the sum throughput of the NOMA users for the buffer-aided cooperative NOMA relay network in [40].

Although there are already many research progresses on buffer-aided techniques, most of the existing work mainly focus on improving the network performance in the single-relay [20], [22], multi-relay [23]–[27], [30]–[33], two-way relay [29], and NOMA-based relaying networks [38]–[40]. The SWIPT technique has not been considered in these works. On the other hand, for most of the existing works about the wireless powered cooperative NOMA relay network, they are dedicated to exploring either the outage performance [6], [11], [12], [34] or the achievable rate [35]. In addition, the long-term power consumption of the NOMA based downlink networks was studied in [36], but the wireless energy transfer was not considered in [36]. Moreover, since we assume that the relay is an energy-constrained node, it can only harvest energy from the source, which makes the optimal transmit power in the energy harvesting phase and the relay transmitting phase become coupled with each other, which poses a technical challenge. To the best of our knowledge, few research efforts are devoted to exploring the buffer-aided mechanism in the wireless powered cooperative NOMA relay networks to improve the realized energy efficiency, which motivates our work in this paper. When the NOMA-based relay is equipped with data buffer and energy storage to store the received data and harvested energy temporarily, three important issues should be addressed: (i) How to design an efficient scheduling scheme to improve energy efficiency? (ii) How the data and energy queues affect the power allocation and transmission mode selection? (iii) Does the data queue affect the NOMA based relaying scheme? These issues motivate our research efforts in this paper.

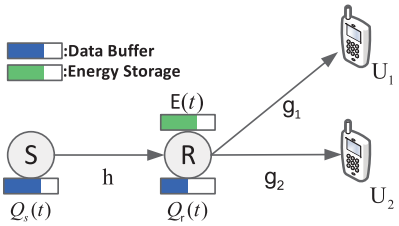

Fig. 1. System model of the NOMA based wireless powered cooperative network.

III. System Model and Energy Efficient Relaying Design

As illustrated in Fig. 1, let us consider a wireless powered cooperative NOMA relay network, in which one source (S) is supposed to send independent messages to two users (U_1, U_2) via one half-duplex energy-constrained decode-and-forward (DF) relay (R). The relay is an energy-constrained node that is powered by RF signal from the source only. It is assumed that there are no direct links between the source and two users. All nodes are assumed to be provisioned with a single antenna. All the underlying wireless channels are assumed to be independent and block fading, such that the channel coefficients remain constant within each time slot but may change independently from one time slot to another. Let $\tilde{h}(t)$ and $\tilde{g}_1(t)$ ($\tilde{g}_2(t)$) denote the channel coefficient of links $S \rightarrow R$ and $R \rightarrow U_1(U_2)$ within the t-th time slot, respectively. Throughout the paper, the perfect CSI is assumed at the source, the relay, and two users. [1] In this paper, the centralized scheduling scheme is assumed, in which the relay is the central control node that keeps track of all the involved CSIs, energy state information (ESI), and buffer state information (BSI). In fact, the relay knows its own BSI and ESI. By designing an appropriate signaling system, the source is assumed to be able to feed its BSI to the relay. The CSI acquisition needs the appropriate channel estimate training/pilot sequence insertion at the transmitter side and the suitable channel estimate design at the receiver side for each communication pair. Since our focus in this paper is on the energy efficient buffer-aided transmission scheme in wireless powered cooperative NOMA relay network, we assume two users can acquire perfect CSI, and feed it back to the relay node. Then the relay node will make the decision on the transmission control at the

[1] Since our focus is the energy efficient wireless powered cooperative NOMA relay network, we do not consider the channel estimation problem in this paper. As for the practical channel estimate design issue in the decode-and-forward relaying system, the readers may refer to the related literature, e.g., [43].

beginning of each time slot, and inform the source how to adapt the transmission and the two users when to receive via the dedicated signaling system. It should be addressed that, although we have assumed ideal CSI acquisitions in our design, it still provides useful guidance on the mechanism design and unveils some insightful philosophy. Of course, all the imperfections, such as the imperfect CSIs, require a robust adaptive relaying scheme that is capable of approaching the performance bound derived in this paper with ideal CSI, which will be left for exploration in the future.

A. Energy Efficient Power Splitting-Based Relaying Design

In the power splitting based relaying protocol, the duration of each time slot T will be sub-divided into two sub-slots. The first $T/2$ is used for relay receiving, and the second $T/2$ is used for information relaying. In the first $T/2$, the power splitting fraction $\rho(t) \in [0,1]$ of the received signal power is used for energy harvesting at R, while the remaining fraction $1-\rho(t)$ of the received signal power is used for relay receiving. Thus the harvested energy at R is

$$E_h(t) = \frac{\rho(t)P(t)|\tilde{h}(t)|^2\eta T}{2d_{sr}^m}, \tag{1}$$

where $P(t)$ is the transmit power by S at time slot t, d_{sr} is the distance between S and R, m is the path loss exponent, and $\eta \in [0,1]$ is the energy conversion efficiency. In the first sub-slot, the received signal at R will be [9]

$$y_r(t) = \sqrt{1-\rho(t)}\Big(\frac{\tilde{h}(t)}{\sqrt{d_{sr}^m}}\sqrt{P(t)}x + n_{r,a}\Big) + n_{r,c}, \tag{2}$$

where x represents the transmitted signal intended for either U_1 or U_2, $\mathbb{E}\{|x|^2\} = 1$. $n_{r,a} \sim \mathcal{CN}(0,\sigma_a^2)$ and $n_{r,c} \sim \mathcal{CN}(0,\sigma_c^2)$ are additive white Gaussian noise (AWGN) at the relay antenna and at the relay down-converter, respectively. Once the channel gain of the link from S to R is given, the maximum transmission rate from S to R is determined accordingly, which equals to $\frac{1}{2}\log_2\Big(1+\frac{(1-\rho(t))P(t)h(t)}{((1-\rho(t))\sigma_a^2+\sigma_c^2)}\Big)$, where $h(t) = \frac{|\tilde{h}(t)|^2}{d_{sr}^m}$. Thus, we can make a transmission rate allocation for two users. Let $R_{si}(t)(i=1,2)$ denote the transmission rate allocated to the message of U_i by the source, which satisfies the following constraint:

$$R_{s1}(t) + R_{s2}(t) \le \tfrac{1}{2}\log_2\Big(1+\frac{(1-\rho(t))P(t)h(t)}{((1-\rho(t))\sigma_a^2+\sigma_c^2)}\Big). \tag{3}$$

After the relay successfully extracts the message for U_1 and U_2, the NOMA based relaying scheme will be used to serve the two users in the remaining time slot, namely, the relay transmits the following mixture signal of x_1 and x_2 via superposition coding,

$$x_r = \sqrt{P_{r1}(t)}x_1 + \sqrt{P_{r2}(t)}x_2, \tag{4}$$

where x_i $(i=1,2)$ is the transmit message intended for U_i, and $\mathbb{E}\{|x_i|^2\} = 1$, $P_{ri}(t)$ is the transmit power for x_i. Thus, the received signal at U_i $(i=1,2)$ is given by

$$y_i(t) = \frac{\tilde{g}_i(t)}{\sqrt{d_{ri}^m}}\Big(\sqrt{P_{r1}(t)}x_1 + \sqrt{P_{r2}(t)}x_2\Big) + n_{i,a} + n_{i,c}, \tag{5}$$

where d_{ri} denotes the distance between R and U_i, $n_{i,a} \sim \mathcal{CN}(0,\sigma_a^2)$ and $n_{i,c} \sim \mathcal{CN}(0,\sigma_c^2)$ are additive white Gaussian noise (AWGN) at the i-th user antenna and at the i-th user down-converter, respectively. Without loss of generality, we assume that $\frac{|\tilde{g}_1(t)|^2}{d_{r1}^m} < \frac{|\tilde{g}_2(t)|^2}{d_{r2}^m}$. According to NOMA scheme, the optimal decoding order for the downlink transmission is ascending order in the channel gain [36], *i.e.*, both users first use successive interference cancellation to decode x_1, and then U_2 subtracts the signal intended for U_1 and decodes its own signal. Let $R_{r1}(t)$ and $R_{r2}(t)$ denote the achievable rate from the relay to U_1 and U_2 at time slot t, respectively, we have

$$R_{r1}(t) = \frac{1}{2}\log_2\Big(1+\frac{P_{r1}(t)g_1(t)}{P_{r2}(t)g_1(t)+\sigma^2}\Big), \tag{6a}$$

$$R_{r2}(t) = \frac{1}{2}\log_2\Big(1+\frac{P_{r2}(t)g_2(t)}{\sigma^2}\Big), \tag{6b}$$

where $g_i(t) = \frac{|\tilde{g}_i(t)|^2}{d_{ri}^m}$ and $\sigma^2 = \sigma_a^2 + \sigma_c^2$. It should be addressed that, the energy consumption of the relay should not exceed its harvested energy, therefore we have

$$P_{r1}(t) + P_{r2}(t) \le \rho(t)P(t)h(t)\eta, \forall t. \tag{7}$$

In this paper, our objective is to minimize the power consumption of the source subject to the minimum required rate by two users. Since the total energy consumption of the source in the t-th time slot is $\frac{P(t)T}{2}$, the average power consumption of the source at time slot t is equal to $\frac{P(t)}{2}$. Thus, the power consumption minimization problem for the PSR protocol can be formulated as follows

$$\begin{aligned}\mathbf{P1}: \ &\min_{P(t),P_{ri}(t),\rho(t)} : \frac{P(t)}{2}\\ &\text{s.t. } \min\{R_{si}(t), R_{ri}(t)\} \ge \bar{R}_i, \ i=1,2,\forall t,\\ &0 \le \rho(t) \le 1, \ \forall t,\\ &(3),(6), \text{and } (7),\end{aligned}$$

where $\bar{R}_i (i=1,2)$ is the minimum required rate by U_i. Unfortunately, the optimization problem **P1** is neither convex nor concave. So it is difficult to directly solve it by using existing optimization tools. However, we can obtain the optimal solution by some analysis and algebraic operations. Firstly, in order to ensure that the relay can harvest enough energy to forward the information to users, we can obtain the minimum required transmit power at the relay by imposing constraints $R_{ri}(t) = \bar{R}_i$ $(i=1,2)$. From (6), the minimum $P_{r1}(t)$ and $P_{r2}(t)$ must satisfy the following equations

$$P_{r1}(t) = (2^{2\bar{R}_1}-1)\Big(\frac{2^{2\bar{R}_2}\sigma^2}{g_2(t)} + \frac{\sigma^2}{g_1(t)} - \frac{\sigma^2}{g_2(t)}\Big), \tag{8a}$$

$$P_{r2}(t) = \frac{(2^{2\bar{R}_2}-1)\sigma^2}{g_2(t)}. \tag{8b}$$

By substituting (8) into (7), we can obtain the minimum required power by the source for a successful transmission from the relay to both users, which is given by

$$f_1^{PS}(\rho(t)) = \frac{\sigma^2}{\rho(t)h(t)\eta}\Big(\frac{2^{2\bar{R}_1}(2^{2\bar{R}_2}-1)}{g_2(t)} + \frac{2^{2\bar{R}_1}-1}{g_1(t)}\Big). \tag{9}$$

Moreover, in order to guarantee that the relay can successfully extract the data of two users, according to (3) and imposing constraints $R_{si}(t) = \bar{R}_i$ $(i = 1, 2)$, we can derive the minimum required transmit power at the source as below

$$f_2^{PS}(\rho(t)) = (2^{2(\bar{R}_1+\bar{R}_2)} - 1)\frac{((1-\rho(t))\sigma_a^2 + \sigma_c^2)}{(1-\rho(t))h(t)}. \quad (10)$$

Thus, **P1** can be transformed into the following single-variable optimization problem:

$$\textbf{P1.1}: \min_{\rho(t)} : \max\{f_1^{PS}(\rho(t)), f_2^{PS}(\rho(t))\} \quad \text{s.t. } 0 \le \rho(t) \le 1.$$

It is worth noting that, $f_1^{PS}(\rho(t))$ and $f_2^{PS}(\rho(t))$ is the monotonically decreasing and increasing function of $\rho(t)$, respectively. Moreover, we can easily derive $\lim_{\rho(t)\to 0} f_1^{PS}(\rho(t)) = \infty$ and $\lim_{\rho(t)\to 1} f_2^{PS}(\rho(t)) = \infty$, which indicates that $f_1^{PS}(\rho(t))$ and $f_2^{PS}(\rho(t))$ have a unique intersection at $\rho(t) \in [0, 1]$. The optimal $\rho(t)$ should satisfy $f_1^{PS}(\rho(t)) = f_2^{PS}(\rho(t))$. One may readily derive that, the optimal $\rho(t)$ satisfies the following equation

$$-\sigma_a^2 A\rho(t)^2 + (\sigma^2 A + B)\rho(t) - B = 0, \quad (11)$$

where $A = (2^{2(\bar{R}_1+\bar{R}_2)} - 1)\eta$ and $B = \frac{2^{2\bar{R}_1}(2^{2\bar{R}_2}-1)\sigma^2}{g_2(t)} + \frac{(2^{2\bar{R}_1}-1)\sigma^2}{g_1(t)}$. Let $f(\rho(t))$ denote the left-hand side of (11). We may easily observe that, $f(0) < 0$ and $f(1) > 0$. Moreover, since $-\sigma_a^2 A < 0$, there must be two roots for (11), one of which satisfies $0 < \rho(t) < 1$, and the other satisfies $\rho(t) > 1$. Thus, we can derive the optimal $\rho(t)$ as follows

$$\rho^*(t) = \frac{\sigma^2 A + B - \sqrt{(\sigma^2 A + B)^2 - 4\sigma_a^2 AB}}{2\sigma_a^2 A}. \quad (12)$$

When we obtain the optimal $\rho^*(t)$, by substituting it into (8) and (10), we can derive the optimal power allocation at R and the minimal power consumption at the source, respectively. In addition, it is worth noting that the optimal power splitting factor $\rho(t)$ for the PSR must satisfy $f_1^{PS}(\rho(t)) = f_2^{PS}(\rho(t))$, $i.e.$, the transmission rate of the first hop equals to that of the second hop, such that no power is wasted. The pseudo-code of the energy efficient PSR design procedure is given in Algorithm 1.

Algorithm 1 Energy Efficient PSR Design Procedure

Input: $h(t), g_1(t), g_2(t), \bar{R}_1, \bar{R}_2, \eta, \sigma_a^2, \sigma_c^2$;
Output: $P^*(t), P_{r1}^*(t), P_{r2}^*(t), \rho^*(t)$;
Set $A = (2^{2(\bar{R}_1+\bar{R}_2)} - 1)\eta$;
if $g_1(t) < g_2(t)$ **then**
  $B = \frac{2^{2\bar{R}_1}(2^{2\bar{R}_2}-1)\sigma^2}{g_2(t)} + \frac{(2^{2\bar{R}_1}-1)\sigma^2}{g_1(t)}$;
  Set $P_{r1}^*(t) = (2^{2\bar{R}_1} - 1)\Big(\frac{2^{2\bar{R}_2}\sigma^2}{g_2(t)} + \frac{\sigma^2}{g_1(t)} - \frac{\sigma^2}{g_2(t)}\Big)$, $P_{r2}^*(t) = \frac{(2^{2\bar{R}_2}-1)\sigma^2}{g_2(t)}$;
else
  Set $B = \frac{2^{2\bar{R}_2}(2^{2\bar{R}_1}-1)\sigma^2}{g_1(t)} + \frac{(2^{2\bar{R}_2}-1)\sigma^2}{g_2(t)}$;
  Set $P_{r1}^*(t) = \frac{(2^{2\bar{R}_1}-1)\sigma^2}{g_1(t)}$, $P_{r2}^*(t) = (2^{2\bar{R}_2} - 1)\Big(\frac{2^{2\bar{R}_1}\sigma^2}{g_1(t)} + \frac{\sigma^2}{g_2(t)} - \frac{\sigma^2}{g_1(t)}\Big)$;
end if
Set $\rho^*(t) = \frac{\sigma^2 A + B - \sqrt{(\sigma^2 A + B)^2 - 4\sigma_a^2 AB}}{2\sigma_a^2 A}$;
Set $P^*(t) = (2^{2(\bar{R}_1+\bar{R}_2)} - 1)\frac{((1-\rho^*(t))\sigma_a^2 + \sigma_c^2)}{(1-\rho^*(t))h(t)}$.

B. Energy Efficient Time Switching-Based Relaying Design

In the time switching based relaying protocol, the duration of each slot will be further sub-divided into three subslots of $\alpha(t)T$, $\frac{(1-\alpha(t))T}{2}$, and $\frac{(1-\alpha(t))T}{2}$, where $\alpha(t) \in [0, 1]$ is the time switching factor. $\alpha(t)T$ is used for the relay to harvest energy from the source, the first $\frac{(1-\alpha(t))T}{2}$ is used for relay receiving, and the remaining $\frac{(1-\alpha(t))T}{2}$ is used for information relaying. So the harvested energy at R in the energy harvesting phase is

$$E_h(t) = \alpha(t)P(t)h(t)\eta T. \quad (13)$$

Like the PSR scheme, we assume that the source transmits a signal x intended for either U_1 or U_2 to R in the relay receiving phase, and the received signal at R can be given by

$$y_r(t) = \frac{\tilde{h}(t)}{\sqrt{d_{sr}^m}}\sqrt{P(t)}x + n_{r,a} + n_{r,c}. \quad (14)$$

Likewise, the achievable rate pair $(R_{s1}(t), R_{s2}(t))$ from S to R satisfies

$$R_{s1}(t) + R_{s2}(t) \le \tfrac{1-\alpha(t)}{2}\log_2\Big(1 + \tfrac{P(t)h(t)}{\sigma^2}\Big). \quad (15)$$

After the relay correctly recovers the data for two users, the relay will use the harvested energy to forward data to two users by using the NOMA scheme. When $g_1(t) < g_2(t)$, the achievable rate from relay to two users can be given by

$$R_{r1}(t) = \frac{1-\alpha(t)}{2}\log_2\Big(1 + \frac{P_{r1}(t)g_1(t)}{P_{r2}(t)g_1(t) + \sigma^2}\Big), \quad (16a)$$

$$R_{r2}(t) = \frac{1-\alpha(t)}{2}\log_2\Big(1 + \frac{P_{r2}(t)g_2(t)}{\sigma^2}\Big). \quad (16b)$$

In addition, due to the energy causality of the relay, the energy used by the relay to forward data should be no larger than its harvested energy, namely,

$$\frac{\big(P_{r1}(t) + P_{r2}(t)\big)(1-\alpha(t))}{2} \le \alpha(t)P(t)h(t)\eta. \quad (17)$$

At time slot t, since the total energy consumed by the source is $\frac{(1+\alpha(t))P(t)T}{2}$, the problem of minimizing the source power consumption in the TSR protocol can be expressed as

$$\textbf{P2}: \min_{P(t),P_{ri}(t),\alpha(t)} : \frac{(1+\alpha(t))P(t)}{2}$$
$$\text{s.t. } \min\{R_{si}(t), R_{ri}(t)\} \ge \bar{R}_i,\ i = 1, 2, \forall t,$$
$$0 \le \alpha(t) \le 1,\ \forall t,$$
$$(15), (16), \text{and } (17).$$

Algorithm 2 Golden Section Search for $\alpha^*(t)$

Input: $h(t), g_1(t), g_2(t), \bar{R}_1, \bar{R}_2, \eta, \sigma^2$, tolerance error ϵ_e;
Output: $\alpha^*(t)$;
Initialization: $a = 0$, $b = 1$, $\alpha_1 = a + 0.382(b-a)$,$\alpha_2 = a + 0.618(b-a)$;
while $\alpha_2 - \alpha_1 > \epsilon_e$ **do**
  Calculate $F(\alpha_1) = \max\{f_1^{TS}(\alpha_1), f_2^{TS}(\alpha_1)\}$ and $F(\alpha_2) = \max\{f_1^{TS}(\alpha_2), f_2^{TS}(\alpha_2)\}$;
  if $F(\alpha_2) > F(\alpha_1)$ **then**
    $b = \alpha_2$, $\alpha_2 = \alpha_1$, and $\alpha_1 = a + 0.382(b-a)$;
  else
    $a = \alpha_1$, $\alpha_1 = \alpha_2$, and $\alpha_2 = a + 0.618(b-a)$;
  end if
end while
Set $\alpha^*(t) = \frac{\alpha_1 + \alpha_2}{2}$.

Like **P1**, **P2** is also non-convex and non-concave. Similarly, by imposing the constraints of $R_{si}(t) = R_{ri}(t) = \bar{R}_i$ $(i = 1, 2)$ and from (16), we can obtain the minimal power requirement for the relay to satisfy the target rate constraints by two users, which are given by

$$P_{r1}(t) = \left(2^{\frac{2\bar{R}_1}{1-\alpha(t)}} - 1\right)\left(\frac{2^{\frac{2\bar{R}_2}{1-\alpha(t)}}\sigma^2}{g_2(t)} + \frac{\sigma^2}{g_1(t)} - \frac{\sigma^2}{g_2(t)}\right), \tag{18a}$$

$$P_{r2}(t) = \frac{\left(2^{\frac{2\bar{R}_2}{1-\alpha(t)}} - 1\right)\sigma^2}{g_2(t)}. \tag{18b}$$

Combined the objective function of **P2** and the energy causality at the relay in (17), to ensure the successful transmission from the relay to users, the minimum required average transmit power at the source should satisfy

$$\begin{aligned} f_1^{TS}(\alpha(t)) &= \frac{(1+\alpha(t))P(t)}{2} \\ &= \frac{1-\alpha^2(t)}{4\alpha(t)h(t)\eta}\left(\frac{2^{\frac{2\bar{R}_1}{1-\alpha(t)}}\left(2^{\frac{2\bar{R}_2}{1-\alpha(t)}} - 1\right)\sigma^2}{g_2(t)}\right. \\ &\quad \left. + \frac{\left(2^{\frac{2\bar{R}_1}{1-\alpha(t)}} - 1\right)\sigma^2}{g_1(t)}\right). \end{aligned} \tag{19}$$

On the other hand, to ensure that the rate from the source to relay can be satisfied, according to (15), we can obtain the minimum required average transmit power by the source as follows

$$\begin{aligned} f_2^{TS}(\alpha(t)) &= \frac{(1+\alpha(t))P(t)}{2} \\ &= \frac{(1+\alpha(t))\left(2^{\frac{2(\bar{R}_1+\bar{R}_2)}{1-\alpha(t)}} - 1\right)\sigma^2}{2h(t)}. \end{aligned} \tag{20}$$

Therefore, **P2** can be equivalently transformed into the following **P2.1**

$$\begin{aligned} \textbf{P2.1}: \ &\min_{\alpha(t)} : \max\{f_1^{TS}(\alpha(t)), f_2^{TS}(\alpha(t))\} \\ &\text{s.t. } 0 \le \alpha(t) \le 1. \end{aligned}$$

Algorithm 3 Energy Efficient TSR Design Procedure

Input: $h(t), g_1(t), g_2(t), \bar{R}_1, \bar{R}_2, \eta, \sigma^2$;
Output: $P^*(t), P_{r1}^*(t), P_{r2}^*(t), \alpha^*(t)$;
Set $f_2^{TS}(\alpha(t)) = \frac{(1+\alpha(t))\left(2^{\frac{2(\bar{R}_1+\bar{R}_2)}{1-\alpha(t)}} - 1\right)\sigma^2}{2h(t)}$;
if $g_1(t) < g_2(t)$ **then**
  Set $f_1^{TS}(\alpha(t))$ $= \frac{1-\alpha^2(t)}{4\alpha(t)h(t)\eta}\left(\frac{2^{\frac{2\bar{R}_1}{1-\alpha(t)}}\left(2^{\frac{2\bar{R}_2}{1-\alpha(t)}} - 1\right)\sigma^2}{g_2(t)} + \frac{\left(2^{\frac{2\bar{R}_1}{1-\alpha(t)}} - 1\right)\sigma^2}{g_1(t)}\right)$;
  Calculate $\alpha^*(t)$, $f_1^{TS}(\alpha^*(t))$, and $f_2^{TS}(\alpha^*(t))$ according to Algorithm 2;
  Set $P_{r1}^*(t) = \left(2^{\frac{2\bar{R}_1}{1-\alpha(t)}} - 1\right)\left(\frac{2^{\frac{2\bar{R}_2}{1-\alpha(t)}}\sigma^2}{g_2(t)} + \frac{\sigma^2}{g_1(t)} - \frac{\sigma^2}{g_2(t)}\right)$, $P_{r2}^*(t) = \frac{\left(2^{\frac{2\bar{R}_2}{1-\alpha(t)}} - 1\right)\sigma^2}{g_2(t)}$;
else
  Set $f_1^{TS}(\alpha(t))$ $= \frac{1-\alpha^2(t)}{4\alpha(t)h(t)\eta}\left(\frac{2^{\frac{2\bar{R}_2}{1-\alpha(t)}}\left(2^{\frac{2\bar{R}_1}{1-\alpha(t)}} - 1\right)\sigma^2}{g_1(t)} + \frac{\left(2^{\frac{2\bar{R}_2}{1-\alpha(t)}} - 1\right)\sigma^2}{g_2(t)}\right)$;
  Calculate $\alpha^*(t)$, $f_1^{TS}(\alpha^*(t))$, and $f_2^{TS}(\alpha^*(t))$ according to Algorithm 2;
  Set $P_{r1}^*(t) = \frac{\left(2^{\frac{2\bar{R}_1}{1-\alpha(t)}} - 1\right)\sigma^2}{g_1(t)}$, $P_{r2}^*(t) = \left(2^{\frac{2\bar{R}_2}{1-\alpha(t)}} - 1\right)\left(\frac{2^{\frac{2\bar{R}_1}{1-\alpha(t)}}\sigma^2}{g_1(t)} + \frac{\sigma^2}{g_2(t)} - \frac{\sigma^2}{g_1(t)}\right)$;
end if
Set $P^*(t) = \frac{2\max\{f_1^{TS}(\alpha^*(t)), f_2^{TS}(\alpha^*(t))\}}{1+\alpha^*(t)}$.

We may easily observe that, **P2.1** is a single-variable optimization problem on $\alpha(t)$, which can be effectively solved by using one-dimension line search algorithms, for instance, the uniform sampling search and the golden section search. In the proposed algorithm, the golden section search is used to derive the optimal $\alpha(t)$, as illustrated in Algorithm 2. Since the search space will be reduced by 38.2% after each iteration in the golden section search procedure and $\alpha(t) \in [0, 1]$, the maximum number of iteration N for the given tolerance error ϵ_e satisfies $0.618^N \le \epsilon_e$, *i.e.*, $N \ge \log(\epsilon_e)/\log(0.618) = 2.0788\log(\frac{1}{\epsilon_e})$. Thus, the computation complexity of Algorithm 2 for calculating $\alpha^*(t)$ is $O(\log(\frac{1}{\epsilon_e}))$.

When the optimal $\alpha^*(t)$ is obtained, by substituting it into (18), we can obtain the optimal power allocation at R. In addition, the optimal transmit power at S can be given by

$$P^*(t) = \frac{2\max\{f_1^{TS}(\alpha^*(t)), f_2^{TS}(\alpha^*(t))\}}{1+\alpha^*(t)}. \tag{21}$$

The pseudo-code of the energy efficient TSR design procedure can be outlined in Algorithm 3.

IV. Adaptive Transmission Design

In this section, we assume that the source is provisioned with a data buffer to store the data from the upper layer application temporarily. The relay is equipped with data buffer and energy storage for temporarily storing the received messages and harvested energy, respectively. The data queue size is assumed to be large enough such that the overflow

probability of data buffer can be negligible.[2] Let $Q_{si}(t)$ and $Q_{ri}(t)$ $(i=1,2)$ denote the amount of data for U_i stored in S and R in time slot t, respectively. Let $E(t)$ denote the available energy in the energy storage at time slot t. The energy storage size is denoted by $\hat{E}$. Unlike the conventional PSR and TSR, when the relay is provisioned with data buffer and energy storage, the entire time slot can be adaptively allocated to the relay for harvesting energy, receiving information, or transmitting data. Thus, we introduce three binary decision variables $q_k(t)=\{0,1\},\ k\in\{1,2,3\}$ to indicate whether or not the corresponding transmission mode is chosen in the t-th time slot. $q_1(t)=1$ if the energy harvesting mode is selected at time slot t, otherwise $q_1(t)=0$. $q_2(t)=1$ $(q_3(t)=1)$ if the relay receiving (transmitting) mode is chosen at time slot t, otherwise $q_2(t)=0$ $(q_3(t)=0)$. In addition, we assume that at most one transmission mode can be selected in each time slot, *i.e.*, $\sum_{k=1}^{3}\ q_k(t)=1$.

A. Problem Formulation

Our objective is to minimize the long-term average power consumption of the source under the constraints of the given target rates by two users, as well as the data and energy queue causality. Moreover, the rate allocation at S, the power allocation at S and R, and transmission mode selection are jointly optimized to minimize the average power consumption of the source. Therefore, the long-term power consumption minimization problem can be formulated as below

$$
\begin{aligned}
\mathbf{P3}:\ \min_{\boldsymbol{R_s},P,\boldsymbol{P_r},\boldsymbol{q}}\ &: \lim_{M\to\infty}\frac{1}{M}\sum_{t=0}^{M-1}P_s(t)\\
\text{s.t. } &C1: Q_{si}(t+1)=\big(Q_{si}(t)+\bar{R}_i-R_{si}(t)\big)^+,\\
&\quad i=1,2,\forall t,\\
&C2: Q_{ri}(t+1)=\big(Q_{ri}(t)+R_{si}(t)-R_{ri}(t)\big)^+,\\
&\quad i=1,2,\forall t,\\
&C3: E(t+1)=\min\big\{\big(E(t)+E_h(t)-E_r(t)\big)^+,\hat{E}\big\},\\
&\quad \forall t,\\
&C4: \lim_{M\to\infty}\frac{1}{M}\sum_{t=0}^{M-1}R_{si}(t)\geq\bar{R}_i, i=1,2,\\
&\quad \lim_{M\to\infty}\frac{1}{M}\sum_{t=0}^{M-1}R_{ri}(t)\geq\lim_{M\to\infty}\frac{1}{M}\sum_{t=0}^{M-1}R_{si}(t), i=1,2,\\
&C5: R_{s1}(t)+R_{s2}(t)\leq q_2(t)\log_2\Big(1+\frac{P(t)h(t)}{\sigma^2}\Big),\forall t,\\
&C6: P(t)\leq\hat{P},\forall t,\\
&C7: P_{r1}(t)+P_{r2}(t)\leq\hat{P}_r(t),\forall t,\\
&C8: q_i(t)\in\{0,1\}, i\in\{1,2,3\},\forall t,\\
&C9: q_1(t)+q_2(t)+q_3(t)=1,\forall t,
\end{aligned}
$$

where $(\cdot)^+\triangleq\max\{\cdot,0\}$ and $P_s(t)=(q_1(t)+q_2(t))P(t)$. The transmission rate pair $(R_{r1}(t),R_{r2}(t))$ is given by

$$
\begin{aligned}
&\big(R_{r1}(t),R_{r2}(t)\big)\\
&=\begin{cases}
q_3(t)\Big(\log_2\Big(1+\dfrac{P_{r1}(t)g_1(t)}{\sigma^2}\Big),\\
\log_2\Big(1+\dfrac{P_{r2}(t)g_2(t)}{P_{r1}(t)g_2(t)+\sigma^2}\Big)\Big), & \text{if } g_1(t)>g_2(t),\\
q_3(t)\Big(\log_2\Big(1+\dfrac{P_{r1}(t)g_1(t)}{P_{r2}(t)g_1(t)+\sigma^2}\Big),\\
\log_2\Big(1+\dfrac{P_{r2}(t)g_2(t)}{\sigma^2}\Big)\Big), & \text{otherwise,}
\end{cases}
\end{aligned}
$$

$E_h(t)$ and $E_r(t)$ denote the harvested energy and consumed energy by R in time slot t, respectively, which are given by

$$E_h(t)=q_1(t)P(t)h(t)\eta T, \tag{22a}$$

$$E_r(t)=q_3(t)(P_{r1}(t)+P_{r2}(t))T. \tag{22b}$$

$\hat{P}$ and $\hat{P}_r(t)$ are the peak transmit power at S and R, respectively. In particular, in each time slot, we set $\hat{P}_r(t)=\frac{E(t)}{T}$ such that the energy consumed by R does not exceed the stored energy. $C1$ and $C2$ represents the data queue causality constraint at S and R, respectively. $C3$ denotes the energy queue evolution constraint. $C4$ represents the target rate constraint of two users. $C5$ ensures that the transmission rate from S to R does not exceed its link capacity. $C6$ and $C7$ stands for the peak transmit power constraint of S and R, respectively. $C8$ and $C9$ specify the transmission mode selection constraint in each time slot.

It is worth noting that the above problem **P3** is a mixed-integer non-convex time average optimization problem. To make the problem more tractable, we transform the time average optimization problem into real-time problem by employing the Lyapunov optimization framework, and decompose it into three subproblems to derive the optimal rate allocation, power allocation, and transmission mode selection separately.

B. Lyapunov Optimization Framework

At first, based on the practical data and energy queue evolution, we can obtain the following Lemma 1.

Lemma 1: If all the data queues of $Q_{si}(t)$ and $Q_{ri}(t)$ $(i=1,2)$ are both rate stable, i.e., $\lim_{M\to\infty}\frac{Q_{si}(M)}{M}=\lim_{M\to\infty}\frac{Q_{ri}(M)}{M}=0$, then we have

$$\lim_{M\to\infty}\frac{1}{M}\sum_{t=0}^{M-1}R_{si}(t)\geq\bar{R}_i, i=1,2, \tag{23a}$$

$$\lim_{M\to\infty}\frac{1}{M}\sum_{t=0}^{M-1}R_{ri}(t)\geq\lim_{M\to\infty}\frac{1}{M}\sum_{t=0}^{M-1}R_{si}(t), i=1,2. \tag{23b}$$

Proof: See Appendix A. ∎

From (23), all the data stored in the data buffer of the source can be successfully sent out if all the data queue are rate stable. This means that, the target rates by both users can be effectively guaranteed, *i.e.*, $C4$ is satisfied. Thus, Lemma 1 indicates that, **P3** can be transformed into minimizing the

[2] In [30], it is shown that, the practical buffer occupancy will be less than the pre-defined control parameter V. Thus it is reasonable to assume no overflow if the storage size is larger than V, which can be adjusted for different traffic delivery delay requirements.

long-term power consumption under the constraints of stabilizing all data queues. The Lyapunov optimization framework can be used to effectively handle this issue.

According to the data and energy queue states, the quadratic Lyapunov function is defined as

$$L(\mathbf{\Theta}(t)) = \frac{1}{2}\sum_{i=1}^{2}\left(Q_{si}^2(t) + Q_{ri}^2(t)\right) + \frac{\mu}{2}(\hat{E} - E(t))^2, \tag{24}$$

where $\mathbf{\Theta}(t) \triangleq [Q_{si}(t), Q_{ri}(t), E(t)]$ denotes the concatenated vector for all involved queues at the beginning of time slot t. μ is a non-negative weighting coefficient for the energy queue, which is used to ensure that the data and energy queue size are in the same order of magnitude. $L(\mathbf{\Theta}(t))$ measures the current backlog of all queues, which grows with the increase in all data queue sizes. The Lyapunov drift specifies the expected change of $L(\mathbf{\Theta}(t))$ between two consecutive slots, which is given by

$$\Delta(\mathbf{\Theta}(t)) = \mathbb{E}[L(\mathbf{\Theta}(t+1)) - L(\mathbf{\Theta}(t))|\mathbf{\Theta}(t)], \tag{25}$$

where the expectation depends on transmission decisions and the randomness of CSI for the given $\mathbf{\Theta}(t)$. To guarantee the stability of all data queues, our transmission decision should minimize the above Lyapunov drift. Meanwhile, our goal is to minimize the long-term power consumption of the source, and thus we can minimize the following Lyapunov drift-plus-penalty

$$\Delta(\mathbf{\Theta}(t)) + V\mathbb{E}[P_s(t)|\mathbf{\Theta}(t)], \tag{26}$$

where $V > 0$ is a non-negative weighting coefficient, which can be set up to effectively realize the tradeoff between the queue stability and the long-term power consumption at S.

Lemma 2: The Lyapunov drift-plus-penalty has the following upper bound,

$$\begin{aligned}\Delta(\mathbf{\Theta}(t)) + V\mathbb{E}[P_s(t)|\mathbf{\Theta}(t)] \le{}& B + V\mathbb{E}[P_s(t)|\mathbf{\Theta}(t)] \\ &+ \sum_{i=1}^{2}\Big\{Q_{si}(t)\mathbb{E}[\bar{R}_i - R_{si}(t)|\mathbf{\Theta}(t)] \\ &+ Q_{ri}(t)\mathbb{E}[R_{si}(t) - R_{ri}(t)|\mathbf{\Theta}(t)]\Big\} \\ &+ \mu(\hat{E} - E(t))\mathbb{E}[E_r(t) - E_h(t)|\mathbf{\Theta}(t)],\end{aligned} \tag{27}$$

where B is a constant independent of V, and $B = \frac{1}{2}\sum_{i=1}^{2}\{2\hat{R}_{si}^2 + \hat{R}_{ri}^2 + \bar{R}_i^2\} + \frac{\mu}{2}(\hat{E}_r^2 + \hat{E}_h^2)$. $\hat{R}_{si}$ and $\hat{R}_{ri}$ denotes the maximum transmission rate of the corresponding link. $\hat{E}_r$ and $\hat{E}_h$ represents the maximum energy consumed and harvested by the relay, respectively.

Proof: See Appendix B. ∎

Lemma 2 gives us the upper bound of the Lyapunov drift-plus-penalty. Here we propose an online rate allocation, power allocation, and transmission mode selection algorithm to minimize the long-term power consumption of the source by minimizing the above upper bound. Given all queue states $\mathbf{\Theta}(t)$ and CSI in each time slot, we make up the transmission decisions on rate and power allocation, as well as transmission mode selection by solving the following real-time optimization problem.

$$\begin{aligned}\mathbf{P3.1}: \min_{\boldsymbol{R_s},P,\boldsymbol{P_r},\boldsymbol{q}} :{}& \sum_{i=1}^{2}\big\{(Q_{ri}(t) - Q_{si}(t))R_{si}(t) - Q_{ri}(t)R_{ri}(t)\big\} \\ &+ \mu(\hat{E} - E(t))(E_r(t) - E_h(t)) + VP_s(t) \\ \text{s.t.}\quad & C5, C6, C7, C8, C9.\end{aligned}$$

Note that the optimization problem **P3.1** is still non-convex. However, we can observe that the optimization variables $q_i(t)$, $(i = 1, 2, 3)$ are binary, and at most one transmission mode can be chosen in each time slot. Therefore, we can enumerate the optimization problem in different situations. If $q_1(t) = 1$, we can derive the optimal power allocation in the energy harvesting mode. If $q_2(t) = 1$, we can design the optimal rate and power allocation of the source in the relay receiving mode. If $q_3(t) = 1$, we can obtain the optimal power allocation of the relay in the relay transmitting mode.

C. Power Allocation in the Energy Harvesting Mode

If the relay is selected to harvest energy from the source, *i.e.*, $q_1(t) = 1$ and $q_2(t) = q_3(t) = 0$, the optimization problem **P3.1** can be equivalently transformed into **P3.2**

$$\begin{aligned}\mathbf{P3.2}: \min_{P(t)} :{}& \big(V - \mu(\hat{E} - E(t))h(t)\eta T\big)P(t) \\ \text{s.t.}\quad & 0 \le P(t) \le \hat{P}.\end{aligned}$$

Apparently, the above optimization problem is a standard linear programming problem, and the optimal solution can be obtained at the boundary only. Thus, we can easily obtain the optimal power allocation of the source in the energy harvesting mode, which is given in Lemma 3.

Lemma 3: The optimal power allocation of the source in the energy harvesting mode is

$$P(t) = \begin{cases}\hat{P}, & \textit{if } \mu(\hat{E} - E(t))h(t)\eta T \ge V, \\ 0, & \textit{otherwise}.\end{cases} \tag{28}$$

From Lemma 3, for a given V, the source transfers energy to the relay with the maximum allowed transmit power only when the channel state $h(t)$ is good enough. Moreover, with the increase in $E(t)$, the probability that the relay can harvest energy from the source will decrease. Furthermore, as V increases, the relay harvests energy only when the channel state $h(t)$ is in a better state.

D. Rate and Power Allocation in the Relay Receiving Mode

If the relay is scheduled to receive messages from the source in time slot t, *i.e.*, $q_2(t) = 1$ and

$$\begin{aligned}\mathbf{P3.3}: \min_{\boldsymbol{R_s},P} :{}& \sum_{i=1}^{2}(Q_{ri}(t) - Q_{si}(t))R_{si}(t) + VP(t) \\ \text{s.t. } & R_{s1}(t) + R_{s2}(t) \le \log_2\Big(1 + \frac{P(t)h(t)}{\sigma^2}\Big), \\ & 0 \le P(t) \le \hat{P}.\end{aligned}$$

Obviously, the objective function of **P3.3** is linear, and all the constraint functions are convex for all optimization variables. Therefore, the above optimization problem is a

standard convex problem. We can easily obtain the optimal rate and power allocation scheme by using the KKT (Karush-Kuhn-Tucher) conditions, which are given in Lemma 4.

Lemma 4: The optimal rate and power allocation scheme of the source in the relay receiving mode can be given by

$$(R_{s1}(t), R_{s2}(t)) = \begin{cases} \left(\log_2\left(1+\frac{P(t)h(t)}{\sigma^2}\right), 0\right), \\ \quad \textit{if } D_1(t) \geq D_2(t) \& D_1(t) > 0, \\ \left(0, \log_2\left(1+\frac{P(t)h(t)}{\sigma^2}\right)\right), \\ \quad \textit{if } D_2(t) \geq D_1(t) \& D_2(t) > 0, \\ (0,0), \\ \quad \textit{otherwise}, \end{cases} \tag{29}$$

$$P(t) = \begin{cases} \min\left(\left(\frac{D_1(t)}{V\ln 2} - \frac{\sigma^2}{h(t)}\right)^+, \hat{P}\right), \\ \quad \textit{if } D_1(t) \geq D_2(t) \& D_1(t) > 0, \\ \min\left(\left(\frac{D_2(t)}{V\ln 2} - \frac{\sigma^2}{h(t)}\right)^+, \hat{P}\right), \\ \quad \textit{if } D_2(t) \geq D_1(t) \& D_2(t) > 0, \\ 0, \\ \quad \textit{otherwise}, \end{cases} \tag{30}$$

where $D_1(t) = Q_{s1}(t) - Q_{r1}(t)$ *and* $D_2(t) = Q_{s2}(t) - Q_{r2}(t)$.

We can observe from Lemma 4 that, unlike the PSR and TSR, at most one user's data will be scheduled to transmit if the current time slot is allocated for relay receiving. That is, with the help of data buffer, the source always allocates the data transmission to the user with the largest data backlog difference between the source buffer backlog $Q_{si}(t)$ and the relay buffer backlog $Q_{ri}(t)$. The data of U_i will not be scheduled for transmission at S as long as the corresponding data backlog $Q_{ri}(t)$ at the relay is larger than $Q_{si}(t)$ at the source. Furthermore, unlike the traditional power water-filling algorithms, the optimal power allocation at S in the relay receiving mode will not only depend on the underlying CSI, but also on the data backlog. A larger $D_i(t)$ will result in a lager allocated power if the data of U_i are scheduled for transmission.

E. Power Allocation in the Relay Transmitting Mode

When the relay is scheduled to transmit the corresponding data to both users by using the NOMA scheme, *i.e.*, $q_1(t) = q_2(t) = 0$ and $q_3(t) = 1$. Without loss of generality, we assume that $g_1(t) < g_2(t)$, and the results can be easily extended to the case of $g_1(t) > g_2(t)$. The optimization problem **P3.3** can be rewritten as below

$$\textbf{P3.4}: \min_{\boldsymbol{P_r}} : -\sum_{i=1}^{2} Q_{ri}(t)R_{ri}(t) + \mu(\hat{E} - E(t))T(P_{r1}(t)+P_{r2}(t))$$

$$\text{s.t. } R_{r1}(t) = \log_2\left(1+\frac{P_{r1}(t)g_1(t)}{P_{r2}(t)g_1(t)+\sigma^2}\right), \tag{31}$$

$$R_{r2}(t) = \log_2\left(1+\frac{P_{r2}(t)g_2(t)}{\sigma^2}\right), \tag{32}$$

$$P_{r1}(t) + P_{r2}(t) \leq \hat{P}_r(t). \tag{33}$$

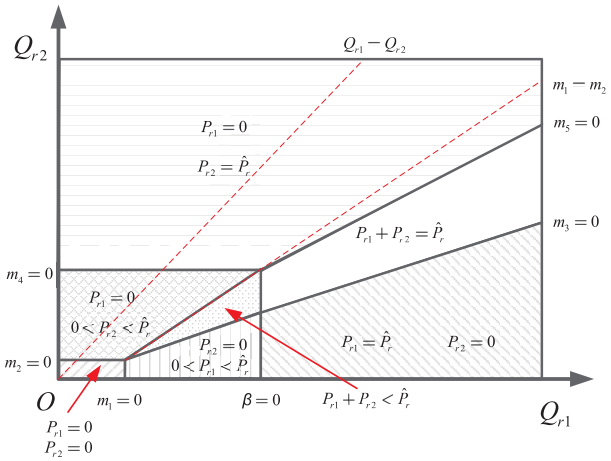

Fig. 2. The optimal transmit power allocation illustration in the relay transmitting mode when $g_1(t) < g_2(t)$.

The above optimization problem is non-convex since both equality constraints are non-linear. However, we can convert **P3.4** into the convex problem by using some mathematical transformation. From (31) and (32), we can obtain

$$P_{r1}(t) = (2^{R_{r1}(t)}-1)\left(\frac{2^{R_{r2}(t)}\sigma^2}{g_2(t)} + \frac{\sigma^2}{g_1(t)} - \frac{\sigma^2}{g_2(t)}\right), \tag{34a}$$

$$P_{r2}(t) = \frac{(2^{R_{r2}(t)}-1)\sigma^2}{g_2(t)}. \tag{34b}$$

By substituting (34) into **P3.4**, we can obtain the following equivalent optimization problem

$$\begin{aligned} \textbf{P3.5}: \quad & \min_{\boldsymbol{R_r}} : -\sum_{i=1}^{2} Q_{ri}(t)R_{ri}(t) + \mu(\hat{E} - E(t))T\sigma^2 \\ & \cdot\left(\frac{2^{R_{r1}(t)+R_{r2}(t)}}{g_2(t)} + \left(\frac{1}{g_1(t)} - \frac{1}{g_2(t)}\right)2^{R_{r1}(t)} - \frac{1}{g_1(t)}\right) \\ & \text{s.t. } \left(\frac{2^{R_{r1}(t)+R_{r2}(t)}}{g_2(t)} + \left(\frac{1}{g_1(t)} - \frac{1}{g_2(t)}\right)2^{R_{r1}(t)} - \frac{1}{g_1(t)}\right) \leq \frac{\hat{P}_r(t)}{\sigma^2}, \\ & R_{ri}(t) \geq 0, i = 1, 2. \end{aligned}$$

We can easily find that the optimization problem **P3.5** is convex when $g_1(t) < g_2(t)$. Hence, we can obtain the optimal rate and power allocation scheme by using the KKT conditions, which are given in Lemma 5.

Lemma 5: The optimal transmission rate pairs $(R_{r1}(t), R_{r2}(t))$ *are given in (35), as shown at the bottom of the next page.*[3] *By substituting them into (34), we can obtain the optimal power allocation scheme in the relay transmitting mode.*

Proof: See Appendix C. ■

[3]Here we drop the time index t for brevity.

In order to gain more insight, the impact of data queue size on the power allocation at the relay is demonstrated in Fig. 2. One may easily observe that, the larger data backlog $Q_{r1}(t)$ and $Q_{r2}(t)$ will lead to larger power consumption, such that the queue stability can be guaranteed. Moreover, if $g_1(t) < g_2(t)$, the relay will use the NOMA scheme to forward the data to both users only when $Q_{r1}(t) > Q_{r2}(t)$. Otherwise, the relay prefers to transmit the data of U_2 only such that the power consumption can be saved. Furthermore, if the data buffer backlog size of U_1 is much larger than that of U_2, to ensure the stability of data queues, the relay tends to only forward the data of U_1 even if its link quality is poor.

F. Transmission Mode Selection

When the optimal power allocation or rate allocation in the corresponding mode have been obtained, by substituting them into the corresponding objective function, we can get the optimal transmission mode selection scheme, which is given in Lemma 6.

Lemma 6: The optimal transmission mode selection scheme is given by

$$q_i^*(t) = \begin{cases} 1, & \text{if } i = \arg\min_{k=1,2,3} \Lambda_k(t), \\ 0, & \text{otherwise}, \end{cases} \tag{36}$$

where $\Lambda_k(t), k = 1, 2, 3$, are the transmission mode selection metrics, which are given by

$$\Lambda_1(t) = \big(V - \mu(\hat{E} - E(t))h(t)\eta T\big)P(t), \tag{37a}$$

$$\Lambda_2(t) = \sum_{i=1}^{2}(Q_{ri}(t) - Q_{si}(t))R_{si}(t) + VP(t), \tag{37b}$$

$$\Lambda_3(t) = \sum_{i=1}^{2}\big(-Q_{ri}(t)R_{ri}(t) + \mu(\hat{E} - E(t))P_{ri}(t)T\big). \tag{37c}$$

From the transmission mode metrics, one may easily observe that, the energy harvesting mode will be scheduled if there is a smaller energy queue size. As the data backlog size at the source $Q_{si}(t)$ increases, the system tends to choose the relay receiving mode such that the data backlog size of relay $Q_{ri}(t)$ will increase. With the increase in $Q_{ri}(t)$, the relay transmitting mode will be scheduled with a higher probability. In the relay transmitting mode, $E(t)$ and $Q_{ri}(t)$ will be decreased until the system goes back to select the energy harvesting mode or relay receiving mode. Therefore, by using the proposed BATS, the stability of data buffers can be guaranteed.

In order to clearly clarify the workflow, the pseudo-code of the proposed BATS is outlined in Algorithm 4.

G. Performance Analysis

In this subsection, we analyze the upper bound of the data queue size and the long-term power consumption of the source achieved by using the proposed BATS.

Theorem 1: When the proposed rate and power allocation, and transmission mode selection scheme are used, for any $V > 0$, there exists $\epsilon > 0$ such that the proposed BATS satisfies the following features:

(1). *All data queue $Q_{si}(t)$ and $Q_{ri}(t)$ ($i = 1, 2$) are rate stable.*

$$(R_{r1}, R_{r2}) = \begin{cases} \left(\log_2\left(\frac{Q_{r1}-Q_{r2}}{(\frac{\sigma^2}{g_1}-\frac{\sigma^2}{g_2})u(\hat{E}-E)T\ln 2}\right), \log_2\left(\frac{Q_{r2}(g_2-g_1)}{(Q_{r1}-Q_{r2})g_1}\right)\right), & \text{if } m_1 > m_2, m_3 > 0, \beta < 0, \\ \left(\log_2\left(\frac{Q_{r1}-Q_{r2}}{(\frac{\sigma^2}{g_1}-\frac{\sigma^2}{g_2})\left(u(\hat{E}-E)T+\beta\right)\ln 2}\right), \log_2\left(\frac{Q_{r2}(g_2-g_1)}{(Q_{r1}-Q_{r2}(t))g_1}\right)\right), & \text{if } m_5 > 0, m_3 > 0, \beta \geq 0, \\ \left(\log_2\left(\frac{Q_{r1}g_1}{\sigma^2 u(\hat{E}-E)T\ln 2}\right), 0\right), & \text{if } m_1 > 0, m_3 \leq 0, \beta < 0, \\ \left(\log_2\left(1+\frac{\hat{P}_r g_1}{\sigma^2}\right), 0\right), & \text{if } m_3 \leq 0, \beta \geq 0, \\ \left(0, \log_2\left(\frac{Q_{r2}g_2}{\sigma^2 u(\hat{E}-E)T\ln 2}\right)\right), & \text{if } m_1 \leq m_2, m_2 > 0, m_4 < 0, \\ \left(0, \log_2\left(1+\frac{\hat{P}_r g_2}{\sigma^2}\right)\right), & \text{if } m_5 \leq 0, m_4 \geq 0, \\ (0,0), & \text{otherwise}, \end{cases} \tag{35}$$

$$m_1 = Q_{r1} - \frac{\sigma^2}{g_1}\mu(\hat{E}-E)T\ln 2, \qquad m_2 = Q_{r2} - \frac{\sigma^2}{g_2}\mu(\hat{E}-E)T\ln 2,$$

$$m_3 = Q_{r2}g_2 - Q_{r1}g_1, \qquad m_4 = Q_{r2} - \Big(\hat{P}_r + \frac{\sigma^2}{g_2}\Big)u(\hat{E}-E)T\ln 2,$$

$$m_5 = Q_{r1}\Big(\hat{P}_r + \frac{\sigma^2}{g_2}\Big) - Q_{r2}\Big(\hat{P}_r + \frac{\sigma^2}{g_1}\Big), \qquad \beta = \frac{Q_{r1}g_1}{(\hat{P}_r g_1 + \sigma^2)\ln 2} - u(\hat{E}-E)T.$$

Algorithm 4 BATS

Input: $h(t), g_1(t), g_2(t), \bar{R}_1, \bar{R}_2, \eta, \sigma^2, T$, and V;
Output: $R^*_{s1}(t), R^*_{s2}(t), P^*(t), P^*_{r1}(t), P^*_{r2}(t)$, and $q^*_k(t)$ $(k = 1, 2, 3)$;
1: Initialization: $Q_{s1}(t) = Q_{s2}(t) = Q_{r1}(t) = Q_{r2}(t) = E(t) = 0$;
2: **for** $t = 1, 2, \ldots, \infty$ **do**
3: Calculate optimal power allocation of the source in the energy harvesting mode based on **Lemma 3**;
4: Calculate the $P^*(t)$, $R^*_{s1}(t)$, and $R^*_{s2}(t)$ in the relay receiving model based on **Lemma 4**;
5: Calculate optimal $P^*_{r1}(t)$ and $P^*_{r2}(t)$ in the relay transmitting mode based on **Lemma 5**;
6: Derive optimal transmission mode selection $q^*_k(t)$ $(k = 1, 2, 3)$ according to **Lemma 6**;
7: Update data queues and the energy queue according to $C1$, $C2$, and $C3$;
8: **end for**

(2). *The average data queue size and average power consumption of the source satisfy the following constraints:*

$$\lim_{M\to\infty} \frac{1}{M} \sum_{t=0}^{M-1} \sum_{i=1}^{2} \mathbb{E}[Q_{si}(t) + Q_{ri}(t)] \leq \frac{B + VP^*_s}{\epsilon}, \tag{38}$$

$$P^*_s \leq \lim_{M\to\infty} \frac{1}{M} \sum_{t=0}^{M-1} \mathbb{E}[P_s(t)] \leq P^*_s + \frac{B}{V}, \tag{39}$$

where P^*_s is a theoretical optimal average power consumption of the source.

Proof: See Appendix D. ∎

From Theorem 1, we can observe that the stability of all data queues can be guaranteed by using the proposed BATS. Combined with Lemma 1, this means that the target rates by two users can be effectively ensured. Moreover, one may easily find that the average data queue size grows linearly with V, and the gap between the long-term power consumption achieved by the proposed BATS and the theoretical optimal value P^*_s is inversely proportional to V. This implies that, the long-term power consumption of the proposed BATS can arbitrarily approach P^*_s at the cost of a large enough average queue size. According to Little's law, the average queueing delay is proportional to the average queueing size. Therefore, we can achieve a tradeoff of $[O(V), O(1/V)]$ between the average queueing delay and the average power consumption.

V. Simulation Results

In this section, we evaluate the performance of the PSR, TSR, and BATS scheme through Monte-Carlo simulations. In all simulations, the data transmission bandwidth is set to be 1 MHz, the noise variance at the antenna and at the down-converter are assumed to $\sigma^2_a = \sigma^2_c = -93$ dBm. The energy storage size is $\hat{E} = 1$ J. The maximum transmit power at the source is $\hat{P} = 2000$ mW. We assume that all links are Rician fading channel, and the Rician factor is set to 10 dB. The path loss exponent is set to be $m = 2.7$. In addition, we assume that the average signal power attenuation is 30 dB at the reference distance of 1 m. Thus, the distance-dependent path loss model is modeled as $PL = 10^{-3} d^{-m}$. The weighting coefficient of energy queue is $\mu = 10^{10}$. The energy conversation efficiency is $\eta = 0.5$. The duration of each time slot is normalized. All the presented simulation results are obtained for $T = 5 \times 10^6$ time slots. Unless otherwise stated, the distance from the source to relay is assumed to $d_{sr} = 5$ m, and the distances from the relay to two users are $d_{r1} = 10$ m and $d_{r2} = 5$ m, respectively.

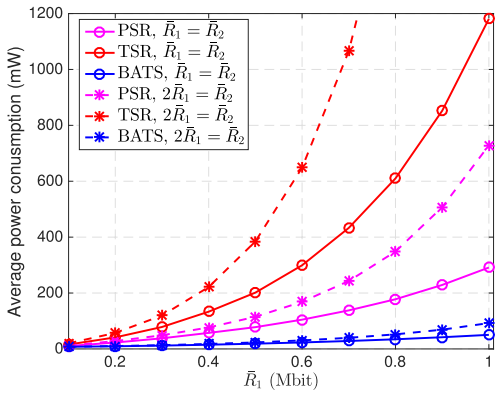

Fig. 3. The average power consumption of the source at different user targeted rates.

Fig. 3 presents the average power consumption of the source for different user target rates. One may easily observe that, the average power consumption in both the PSR and TSR scheme dramatically increases with the increase in the user target rate. However, the average power consumption growth of the BATS scheme is relatively slow. Moreover, we can find that the PSR outperforms the TSR in terms of energy efficiency, and the performance of the BATS is noticeably superior to the PSR and TSR. This can be explained as follows: (i) Based on the previous analysis in Section III, when compared with the TSR, the optimal power splitting factor $\rho(t)$ for the PSR must satisfy $f^{PS}_1(\rho(t)) = f^{PS}_2(\rho(t))$, *i.e.*, the transmission rate of the first hop equals to that of the second hop, such that no power is wasted. (ii) In the BATS, benefiting from the advantages of the data buffer and energy storage, the system can adaptively decide the mode selection based on the current queue length and CSIs, which results in significant improvements in terms of the realized energy efficiency and the time diversity gain.

To explore the effect of target rate changes on the queue length for the BATS, we present the time evolution of the energy queue size, the data queue size, and the transmission rate from the relay to two users in Fig. 4. At the initial time, the targeted rates are $\bar{R}_1 = \bar{R}_2 = 0.5$ Mbps. At time $t = 10^6$, the target rates are changed to $\bar{R}_1 = \bar{R}_2 = 1$ Mbps. At time $t = 3 \times 10^6$, the target rate of U_2 increases to $\bar{R}_2 = 2$ Mbps. We can find that both energy and queue sizes will quickly enter a new stable state when the target rates are changed, which indicates that the BATS can effectively ensure the stability of all queues. Moreover, with the increase in target rates, energy queue size will decrease, and data queue size will increase. Furthermore, as shown in Fig. 4(c), the user rate requirements can be quickly fulfilled when the target rates change.

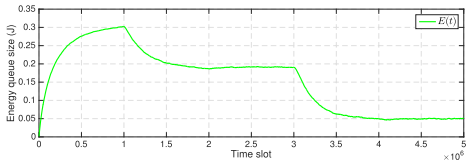

(a) The time evoltution of the energy queue size.

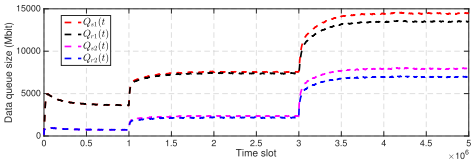

(b) The time evolution of the data queue size.

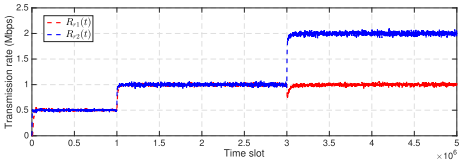

(c) The time evolution of the transmission rate from the relay to two users.

Fig. 4. The time evolution of the energy queue size, the data queue size, and the transmission rate.

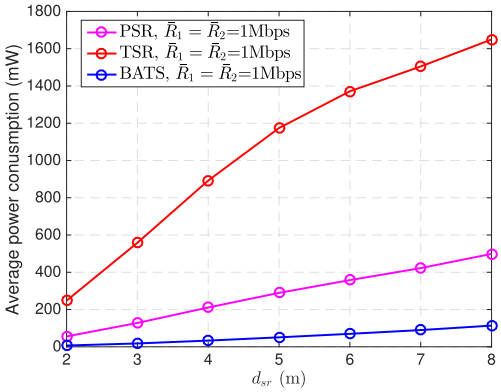

Fig. 5. Average power consumption of the source v.s. d_{sr}.

Fig. 5 presents the effect of the relay location on the average power consumption of the source. Here, we assume that the source, the relay, and U_2 are on the same horizontal line. U_1 is located in the vertical direction of U_2 and is 8.66m away from U_2. The distance between the source and U_2 is fixed at 10 m. It can be easily observed that, the average power consumption of the source will increase as the distance between the source and the relay increases, which complies with the heuristics that, the power consumption can be reduced if the relay is closer to the source.

With different values of V, the average power consumption of the source in the energy harvesting mode and relay receiving mode are presented in Fig. 6. We can observe that, both average power consumption for energy harvesting and data transmission will decrease with the increase in V. However, the average power consumption for data transmission is reduced to a certain value and will not continue to decline. This is because the amount of transmitted data is fixed when the target rates are given. Moreover, we can find that the average

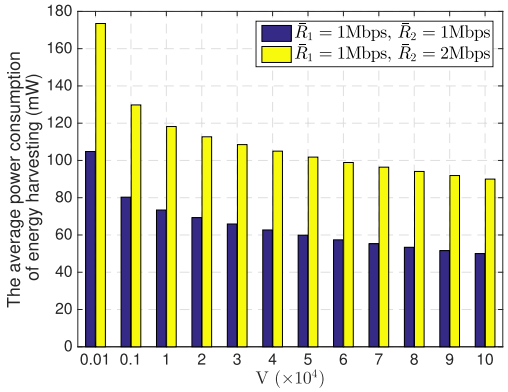

(a) The average power consumption for energy harvesting.

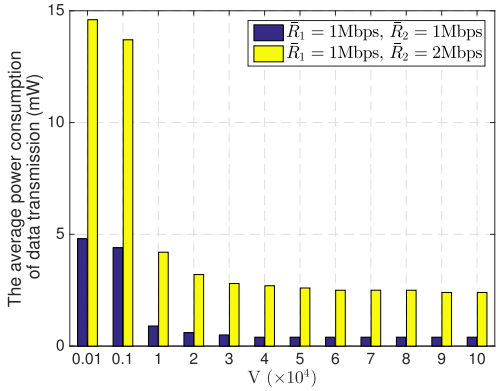

(b) The average power consumption for data transmission.

Fig. 6. The average power consumption for energy harvesting and data transmission with different V.

power consumption used for energy harvesting is much larger than that for data transmission. This can be interpreted by the fact that, the relay is an energy-constrained node and its harvested energy decays exponentially with distance. In order to ensure successful transmission of the second hop, the relay has to harvest enough energy, resulting in larger power consumption in the energy harvesting mode.

The effect of different choices of V on the average data queue size and average power consumption for the BATS are shown in Fig. 7(a) and Fig. 7(b), respectively. We can find that the average queue length of data buffers are proportional to the value of V. Moreover, the average power consumption of the source decreases as the value of V increases. However, it is worth noting that only a slight amount of transmitting power can be saved when V is large enough. All of these simulation results are consistent with Theorem 1. The relationship between the average queueing delay and V is presented in Fig. 7(c). We can observe that, the average queueing delay increases with the increase in V, which indicates that we can set an appropriate value of V based on the user's sensitivity to the delay to ensure its delay requirement. Moreover, U_2 has a lower average queueing delay than that of U_1. This is because U_2 is closer to the relay and it can achieve a larger transmission rate. Furthermore, combined with Fig.7(b), we can conclude that, if users can accept larger queueing delay, user target rates can be satisfied with less power consumption.

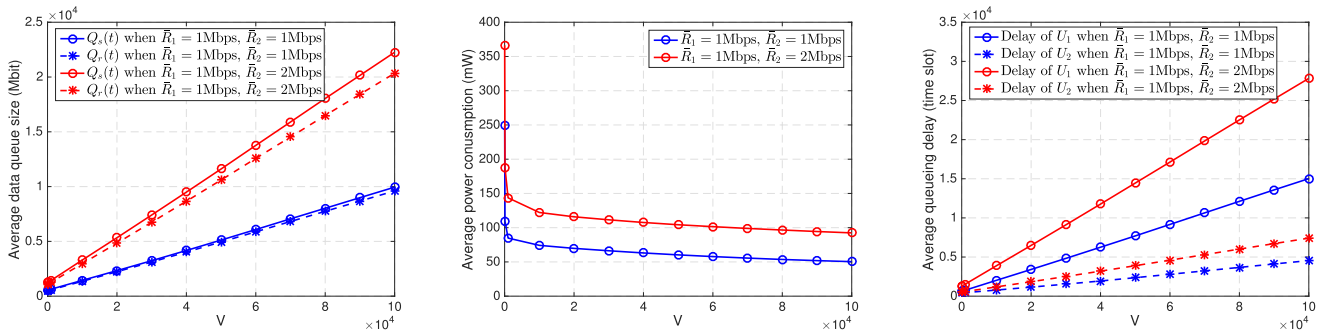

(a) The average data queue size with different choice of V.

(b) The average power consumption with different choice of V.

(c) The average data queueing delay with different choice of V.

Fig. 7. The average data queue size, average power consumption, and average queueing delay with different V.

VI. Conclusion

In this paper, we study the power consumption minimum problem for the wireless powered cooperative NOMA networks, where a source communicates with two users via an energy-constrained relay, and the NOMA scheme is used for forwarding data to both users. First, we derive the minimum power consumption for the conventional PSR and TSR without buffering. Moreover, we formulate the long-term average power consumption minimization problem when the relay is equipped with data buffer and energy storage, which considers the data queue and energy queue causality, peak transmit constraint, and transmission mode selection. By transforming the long-term optimization problem into real-time one, we proposed a novel BATS scheme and proved that the proposed BATS can provide us asymptotically optimal solution. Furthermore, simulation results reveal that, PSR outperforms TSR in terms of the realized energy efficiency. Compared with TSR and PSR, the proposed BATS can significantly improve energy efficiency due to the advantage of buffer-aided transmission mechanism. Finally, in the realistic scenarios, the obtained CSI may be imperfect, and we need to design a robust transmission scheme, which will be explored in our future work. Moreover, it should be addressed that, in this paper, the required energy consumption for transmitting training pilots for channel estimate at the source and relay, as well as the required energy consumption for the CSI feedback by two users to the relay and the control decision transmission from the relay to the source and two users via the dedicated control signalling system is not considered. When the aforementioned energy consumption becomes non-negligible, there should be some increase in the required energy consumption at the relay and the source. We leave this practical analysis in our future work as well.

Appendix A
Proof of Lemma 1

Based on the data queue evolution in $C1$ and $C2$ of the optimization problem **P3**, we have

$$Q_{si}(t+1) \geq Q_{si}(t) + \bar{R}_i - R_{si}(t),\ i = 1, 2, \forall t, \quad (40a)$$

$$Q_{ri}(t+1) \geq Q_{ri}(t) + R_{si}(t) - R_{ri}(t),\ i = 1, 2, \forall t. \quad (40b)$$

By summing the above equations from 0 to $M-1$, dividing it by M and taking limit, we have

$$\lim_{M\to\infty} \frac{Q_{si}(M) - Q_{si}(0)}{M} \geq \bar{R}_i - \lim_{M\to\infty} \frac{1}{M} \sum_{t=0}^{M-1} R_{si}(t), \quad (41a)$$

$$\lim_{M\to\infty} \frac{Q_{ri}(M) - Q_{ri}(0)}{M} \geq \lim_{M\to\infty} \frac{1}{M} \sum_{t=0}^{M-1} \big(R_{si}(t) - R_{ri}(t)\big). \quad (41b)$$

Without loss of generality, we assume that the initial states of data queues are zero, *i.e.*, $Q_{si}(0) = Q_{ri}(0) = 0$. Since all data queues are rate stable, *i.e.*, $\lim_{M\to\infty} \frac{Q_{si}(M)}{M} = \lim_{M\to\infty} \frac{Q_{ri}(M)}{M} = 0$, by substituting them into (41), we can obtain the Lemma 1.

Appendix B
Proof of Lemma 2

According to data and energy queue evolutions in **P3**, for each time slot, we have

$$Q_{si}^2(t+1) \leq Q_{si}^2(t) + 2(\bar{R}_i - R_{si}(t))Q_{si}(t) + \bar{R}_i^2 + \hat{R}_{si}^2,$$
$$Q_{ri}^2(t+1) \leq Q_{ri}^2(t) + 2(R_{ri}(t) - R_{si}(t))Q_{si}(t) + \hat{R}_{ri}^2 + \hat{R}_{si}^2,$$
$$(\hat{E} - E(t+1))^2 \leq (\hat{E} - E(t))^2$$
$$+ 2(\hat{E} - E(t))(E_r(t) - E_h(t)) + \hat{E}_r^2 + \hat{E}_h^2.$$

Substitute the above equations into (26), we can obtain the Lemma 2.

Appendix C
Proof of Lemma 5

Since the proposed algorithm for deriving the power allocation of the relay is to solve the optimization problem **P3.4**, which is non-convex. However, we have equivalently transformed **P3.4** into the convex problem, *i.e.*, **P3.5**. Thus, we can use KKT conditions to obtain the optimal solution, and the corresponding Lagrange function is where $\beta(t) \geq 0$ and $\beta_i(t) \geq 0$ $(i = 1, 2)$ are Lagrange multipliers associated with constraint conditions of **P3.5**. According to the KKT

conditions, we have.[4]

$$\frac{\partial L}{\partial R_{r1}} = \big(\mu(\hat{E}-E)T+\beta\big)\sigma^2\Bigg(\frac{2^{R_{r1}+R_{r2}}}{g_2} + \Big(\frac{1}{g_1}-\frac{1}{g_2}\Big)2^{R_{r1}}\Bigg)\ln 2 - Q_{r1} - \beta_1 = 0, \tag{43}$$

$$\frac{\partial L}{\partial R_{r2}} = \big(\mu(\hat{E}-E)T+\beta\big)\sigma^2\frac{2^{R_{r1}+R_{r2}}}{g_2}\ln 2 - Q_{r2} - \beta_2 = 0, \tag{44}$$

$$\beta\Bigg(\sigma^2\Bigg(\frac{2^{R_{r1}+R_{r2}}}{g_2}+\Big(\frac{1}{g_1}-\frac{1}{g_2}\Big)2^{R_{r1}}-\frac{1}{g_1}\Bigg) - \hat{P}_r\Bigg) = 0, \tag{45}$$

$$\beta_i R_{ri} = 0,\ i = 1, 2. \tag{46}$$

Based on the possible value of transmission rate (R_{r1}, R_{r2}), we can divide it into four cases and discuss them separately.

Case 1: If $R_{r1} > 0$ and $R_{r2} > 0$, we can obtain $\beta_1 = \beta_2 = 0$. By substituting (44) into (43), we can obtain the optimal transmission rates in this case, which are given by

$$R_{r1} = \log_2\Bigg(\frac{Q_{r1}-Q_{r2}}{(\frac{\sigma^2}{g_1}-\frac{\sigma^2}{g_2})(u(\hat{E}-E)T+\beta)\ln 2}\Bigg), \tag{47a}$$

$$R_{2r} = \log_2\Bigg(\frac{Q_{r2}(g_2-g_1)}{(Q_{r1}-Q_{r2})g_1}\Bigg). \tag{47b}$$

In addition, if $\sigma^2\Bigg(\frac{2^{R_{r1}+R_{r2}}}{g_2}+\Big(\frac{1}{g_1}-\frac{1}{g_2}\Big)2^{R_{r1}}-\frac{1}{g_1}\Bigg) = \hat{P}_r$, we have $\beta \geq 0$, otherwise $\beta = 0$. If $\beta \geq 0$, we can substitute (47a) into (45) to obtain the value of β, which is given by

$$\beta = \frac{Q_{r1}g_1}{(\hat{P}_r g_1+\sigma^2)\ln 2} - u(\hat{E}-E)T. \tag{48}$$

If $\beta = 0$, the optimal (R_{r1}, R_{r2}) must satisfy $\sigma^2\Bigg(\frac{2^{R_{r1}+R_{r2}}}{g_2}+\Big(\frac{1}{g_1}-\frac{1}{g_2}\Big)2^{R_{r1}}-\frac{1}{g_1}\Bigg) < \hat{P}_r$. According to the above discussion and set $R_{1r} > 0$ and $R_{2r} > 0$, we can obtain the necessary and sufficient condition that the optimal solution satisfies this case.

Case 2: If $R_{r1} > 0$ and $R_{r2} = 0$, we have $\beta_1 = 0$ and $\beta_2 \geq 0$. From (43), we can obtain the optimal R_{r1} in this case, which is given by

$$R_{r1} = \log_2\Bigg(\frac{Q_{r1}g_1}{\sigma^2(u(\hat{E}-E)T+\beta)\ln 2}\Bigg). \tag{49}$$

If $\frac{(2^{R_{r1}}-1)\sigma^2}{g_1} = \hat{P}_r$, we have $\beta \geq 0$, otherwise $\beta = 0$. When $\beta \geq 0$, by substituting (49) into (45), we can derive β, which is given in (48). When $R_{r2} = 0$, we can derive the value of β_2 from (44). Based on the above discussion and set $R_{1r} > 0$ and $\beta_2 \geq 0$, we can obtain the necessary and sufficient condition that the optimal solution satisfies $R_{r1} > 0$ and $R_{r2} = 0$.

Case 3: If $R_{r1} = 0$ and $R_{r2} > 0$, we have $\beta_1 \geq 0$ and $\beta_2 = 0$. The similar process with *Case 2* can be performed in this case. Here we omit it to save space.

Case 4: If $R_{r1} = R_{r2} = 0$, we can yield $\beta_1 \geq 0$, $\beta_2 \geq 0$, and $\beta = 0$. By substituting $R_{r1} = R_{r2} = 0$ into (43) and (44), we can obtain the values of β_1 and β_2. By setting $\beta_1 \geq 0$, $\beta_2 \geq 0$, we can obtain the necessary and sufficient condition for the case $R_{r1} = R_{r2} = 0$.

Summarize all cases, we can conclude Lemma 5.

APPENDIX D
PROOF OF THEOREM 1

For the considered optimization problem **P3**, there exists a stationary randomized rate and power allocation, and mode selection policy $(\tilde{\boldsymbol{R}}_{\boldsymbol{s}}(t), \tilde{P}(t), \tilde{\boldsymbol{P}}_r(t), \tilde{\boldsymbol{q}}(t))$ that is independent of current data and energy queue with following properties [42]

$$\begin{aligned}\mathbb{E}[\tilde{P}_s(t)|\boldsymbol{\Theta}(t)] &= \mathbb{E}[\tilde{P}_s(t)] = P_s^*,\\ \mathbb{E}[\bar{R}_i - \tilde{R}_{si}(t)|\boldsymbol{\Theta}] &= \mathbb{E}[\bar{R}_i - \tilde{R}_{si}(t)] \leq -\epsilon, i = 1, 2,\\ \mathbb{E}[\tilde{R}_{si}(t) - \tilde{R}_{ri}(t)|\boldsymbol{\Theta}] &= \mathbb{E}[\bar{R}_{si}(t) - \tilde{R}_{ri}(t)] \leq -\epsilon, i = 1, 2.\end{aligned}$$

Since the proposed BATS $(\boldsymbol{R}_{\boldsymbol{s}}(t), P(t), \boldsymbol{P}_r(t), \boldsymbol{q}(t))$ is to minimize the upper bound of the Lyapunov drift-plus-penalty, and the average energy consumption of the relay for any scheduling scheme cannot exceed its harvested energy, substituting the above equations into (27), we have

$$\Delta(\boldsymbol{\Theta}(t)) + V\mathbb{E}[P_s(t)|\boldsymbol{\Theta}(t)] \leq B + VP_s^* - \epsilon\sum_{i=1}^{2}\big(Q_{si}(t)+Q_{ri}(t)\big). \tag{50}$$

Taking expectations for (50), we can yield

$$\mathbb{E}[L(\boldsymbol{\Theta}(t+1)) - L(\boldsymbol{\Theta}(t))] + V\mathbb{E}[P_s(t)] \leq B + VP_s^* - \epsilon\sum_{i=1}^{2}\mathbb{E}[Q_{si}(t)+Q_{ri}(t)]. \tag{51}$$

Without loss of generality, we assume that the initial queue states of all queues are zero, i.e., $L(\boldsymbol{\Theta}(0)) = 0$. Thus, summing the above equation from 0 to $M-1$, we have

$$\frac{1}{2}\sum_{i=1}^{2}\big(\mathbb{E}[Q_{si}^2(M)] + \mathbb{E}[Q_{ri}^2(M)]\big) \leq BM + VP_s^*M. \tag{52}$$

[4]Here we drop the time index for brevity.

$$\mathcal{L}(\boldsymbol{R}_{\boldsymbol{s}}, \boldsymbol{\beta}) = -\sum_{i=1}^{2}Q_{ri}(t)R_{ri}(t) + \big(\mu(\hat{E}-E(t))T+\beta(t)\big)\sigma^2\Bigg(\frac{2^{R_{r1}(t)+R_{r2}(t)}}{g_2(t)} + \Big(\frac{1}{g_1(t)}-\frac{1}{g_2(t)}\Big)2^{R_{r1}(t)} - \frac{1}{g_1(t)}\Bigg) - \beta(t)\hat{P}_r(t) - \sum_{i=1}^{2}\beta_i(t)R_{ri}(t). \tag{42}$$

Due to the fact that $\mathbb{E}[Q^2(t)] \geq \mathbb{E}[Q(t)]^2$, from (52), we have

$$\mathbb{E}[Q_{si}(M)] \leq \sqrt{2M(B + VP_s^*)},\ i = 1, 2. \tag{53}$$

Dividing by M and taking the limit as $M \to \infty$ for (53), we can yield $\lim_{M\to\infty} \frac{\mathbb{E}[Q_{si}(M)]}{M} = 0$. Similar processes can be used to data queues of the relay, and thus all queues are rate stable.

On the other hand, by summing (51) from 0 to $M-1$ slots and dividing it by M, we have

$$\frac{\mathbb{E}[L(\mathbf{\Theta}(M))] - \mathbb{E}[L(\mathbf{\Theta}(0))]}{M} + \frac{V}{M}\sum_{t=0}^{M-1}\mathbb{E}[P_s(t)]$$
$$\leq B + VP_s^* - \frac{\epsilon}{M}\sum_{t=0}^{M-1}\sum_{i=1}^{2}\mathbb{E}[Q_{si}(t) + Q_{ri}(t)] \tag{54}$$

Since $L(\mathbf{\Theta}(0)) \geq 0$, we can yield

$$\frac{1}{M}\sum_{t=0}^{M-1}\mathbb{E}[P_s(t)] \leq \frac{B}{V} + P_s^*, \tag{55}$$

$$\frac{1}{M}\sum_{t=0}^{M-1}\sum_{i=1}^{2}\mathbb{E}[Q_{si}(t) + Q_{ri}(t)] \leq \frac{B + VP_s^*}{\epsilon}. \tag{56}$$

By taking the limit as $M \to \infty$ for above equations, we can conclude the Theorem 1.

REFERENCES

[1] L. Dai, B. Wang, Y. Yuan, S. Han, C.-L. I, and Z. Wang, "Non-orthogonal multiple access for 5G: Solutions, challenges, opportunities, and future research trends," *IEEE Commun. Mag.*, vol. 53, no. 9, pp. 74–81, Sep. 2015.

[2] Z. Ding, Z. Yang, P. Fan, and H. V. Poor, "On the performance of non-orthogonal multiple access in 5G systems with randomly deployed users," *IEEE Signal Process. Lett.*, vol. 21, no. 12, pp. 1501–1505, Dec. 2014.

[3] Z. Ding, X. Lei, G. K. Karagiannidis, R. Schober, J. Yuan, and V. Bhargava, "A survey on non-orthogonal multiple access for 5G networks: Research challenges and future trends," *IEEE J. Sel. Areas Commun.*, vol. 35, no. 10, pp. 2181–2195, Oct. 2017.

[4] Z. Zhang, Z. Ma, X. Lei, M. Xiao, C.-X. Wang, and P. Fan, "Power domain non-orthogonal transmission for cellular mobile broadcasting: Basic scheme, system design, and coverage performance," *IEEE Wireless Commun.*, vol. 25, no. 2, pp. 90–99, Apr. 2018.

[5] X. Chen, F.-K. Gong, G. Li, H. Zhang, and P. Song, "User pairing and pair scheduling in massive MIMO-NOMA systems," *IEEE Commun. Lett.*, vol. 22, no. 4, pp. 788–791, Apr. 2018.

[6] Z. Yang, Z. Ding, P. Fan, and N. Al-Dhahir, "The impact of power allocation on cooperative non-orthogonal multiple access networks with SWIPT," *IEEE Trans. Wireless Commun.*, vol. 16, no. 7, pp. 4332–4343, Jul. 2017.

[7] X. Lu, D. Niyato, P. Wang, D. I. Kim, and Z. Han, "Wireless charger networking for mobile devices: Fundamentals, standards, and applications," *IEEE Wireless Commun.*, vol. 22, no. 2, pp. 126–135, Apr. 2015.

[8] X. Zhou, R. Zhang, and C. K. Ho, "Wireless information and power transfer: Architecture design and rate-energy tradeoff," *IEEE Trans. Commun.*, vol. 61, no. 11, pp. 4754–4767, Nov. 2013.

[9] A. A. Nasir, X. Zhou, S. Durrani, and R. A. Kennedy, "Relaying protocols for wireless energy harvesting and information processing," *IEEE Trans. Wireless Commun.*, vol. 12, no. 7, pp. 3622–3636, Jul. 2013.

[10] X. Li, J. Li, and L. Li, "Performance analysis of impaired SWIPT NOMA relaying networks over imperfect weibull channels," *IEEE Syst. J.*, to be published, doi: 10.1109/JSYST.2019.2919654.

[11] Y. Zhang and J. Ge, "Impact analysis for user pairing on NOMA-based energy harvesting relaying networks with imperfect CSI," *IET Commun.*, vol. 12, no. 13, pp. 1609–1614, 2018.

[12] T. Nguyen and D. Do, "Power allocation schemes for wireless powered NOMA systems with imperfect CSI: An application in multiple antenna-based relay," *Int. J. Commun. Syst.*, vol. 13, no. 15, 2018, Art. no. e3789.

[13] Y. Xu *et al.*, "Joint beamforming and power-splitting control in downlink cooperative SWIPT NOMA systems," *IEEE Trans. Signal Process.*, vol. 65, no. 18, pp. 4874–4886, Sep. 2017.

[14] Y. Liu, Z. Ding, M. Elkashlan, and H. V. Poor, "Cooperative non-orthogonal multiple access with simultaneous wireless information and power transfer," *IEEE J. Sel. Areas Commun.*, vol. 34, no. 4, pp. 938–953, Apr. 2016.

[15] Z. Yang, Z. Ding, Y. Wu, and P. Fan, "Novel relay selection strategies for cooperative NOMA," *IEEE Trans. Veh. Technol.*, vol. 66, no. 11, pp. 10114–10123, Nov. 2017.

[16] Z. Ding, H. Dai, and H. V. Poor, "Relay selection for cooperative NOMA," *IEEE Wireless Commun. Lett.*, vol. 5, no. 4, pp. 416–419, Aug. 2016.

[17] P. Xu, Z. Yang, Z. Ding, and Z. Zhang, "Optimal relay selection schemes for cooperative NOMA," *IEEE Trans. Veh. Technol.*, vol. 67, no. 8, pp. 7851–7855, Aug. 2018.

[18] D. Deng, L. Fan, X. Lei, W. Tan, and D. Xie, "Joint user and relay selection for cooperative NOMA networks," *IEEE Access*, vol. 5, pp. 20220–20227, 2017.

[19] X. Liang, Y. Wu, D. W. K. Ng, Y. Zuo, S. Jin, and H. Zhu, "Outage performance for cooperative NOMA transmission with an AF relay," *IEEE Commun. Lett.*, vol. 21, no. 11, pp. 2428–2431, Nov. 2017.

[20] N. Zlatanov, R. Schober, and P. Popovski, "Buffer-aided relaying with adaptive link selection," *IEEE J. Sel. Areas Commun.*, vol. 31, no. 8, pp. 1530–1542, Aug. 2013.

[21] X. Lan, Q. Chen, X. Tang, and L. Cai, "Achievable rate region of the buffer-aided two-way energy harvesting relay network," *IEEE Trans. Veh. Technol.*, vol. 67, no. 11, pp. 11127–11142, Nov. 2018.

[22] M. M. Razlighi and N. Zlatanov, "Buffer-aided relaying for the two-hop full-duplex relay channel with self-interference," *IEEE Trans. Wireless Commun.*, vol. 17, no. 1, pp. 477–491, Jan. 2018.

[23] N. Nomikos, T. Charalambous, I. Krikidis, D. N. Skoutas, D. Vouyioukas, and M. Johansson, "A buffer-aided successive opportunistic relay selection scheme with power adaptation and inter-relay interference cancellation for cooperative diversity systems," *IEEE Trans. Commun.*, vol. 63, no. 5, pp. 1623–1634, May 2015.

[24] F. L. Duarte and R. C. de Lamare, "Buffer-aided max-link relay selection for multi-way cooperative multi-antenna systems," *IEEE Commun. Lett.*, vol. 23, no. 8, pp. 1423–1426, Aug. 2019.

[25] T. Peng and R. C. de Lamare, "Adaptive buffer-aided distributed space-time coding for cooperative wireless networks," *IEEE Trans. Commun.*, vol. 64, no. 5, pp. 1888–1900, May 2016.

[26] J. Gu, R. C. de Lamare, and M. Huemer, "Buffer-aided physical-layer network coding with optimal linear code designs for cooperative networks," *IEEE Trans. Commun.*, vol. 66, no. 6, pp. 2560–2575, Jun. 2018.

[27] Y. Gong, G. Chen, and T. Xie, "Using buffers in trust-aware relay selection networks with spatially random relays," *IEEE Trans. Wireless Commun.*, vol. 17, no. 9, pp. 5818–5826, Jul. 2018.

[28] H. Saki, T. Peng, and M. S. Bahae, "Energy efficient delay sensitive optimization in SWIPT-MIMO," in *Proc. IEEE GLOBECOM*, Dec. 2018, pp. 1–7.

[29] V. Jamali, N. Zlatanov, A. Ikhlef, and R. Schober, "Achievable rate region of the bidirectional buffer-aided relay channel with block fading," *IEEE Trans. Inf. Theory*, vol. 60, no. 11, pp. 7090–7111, Nov. 2014.

[30] Y. Liu, Q. Chen, X. Tang, and L. X. Cai, "On the buffer energy aware adaptive relaying in multiple relay network," *IEEE Trans. Wireless Commun.*, vol. 16, no. 9, pp. 6248–6263, Sep. 2017.

[31] A. Ikhlef, D. S. Michalopoulos, and R. Schober, "Max-max relay selection for relays with buffers," *IEEE Trans. Wireless Commun.*, vol. 11, no. 3, pp. 1124–1135, Mar. 2012.

[32] N. Zlatanov, V. Jamali, and R. Schober, "Achievable rates for the fading half-duplex single relay selection network using buffer-aided relaying," *IEEE Trans. Wireless Commun.*, vol. 14, no. 8, pp. 4494–4507, Aug. 2015.

[33] Q. Wang, P. Fan, M. R. Mckay, and K. B. Letaief, "On the position selection of relays in diamond relay networks," *IEEE Trans. Commun.*, vol. 59, no. 9, pp. 2515–2527, Sep. 2011.

[34] D. Do, M. Vaezi, and T. Nguyen, "Wireless powered cooperative relaying using NOMA with imperfect CSI," in *Proc. IEEE Globecom Workshops*, Dec. 2018, pp. 1–6.

[35] Y. Yuan, P. Xu, Z. Yang, Z. Ding, and Q. Chen, "Joint robust beamforming and power-splitting ratio design in SWIPT-based cooperative NOMA systems with CSI uncertainty," *IEEE Trans. Veh. Technol.*, vol. 68, no. 3, pp. 2386–2400, Mar. 2019.

[36] D. Zhai, R. Zhang, L. Cai, B. Li, and Y. Jiang, "Energy-efficient user scheduling and power allocation for NOMA-based wireless networks with massive IoT devices," *IEEE Internet Things J.*, vol. 5, no. 3, pp. 1857–1868, Jun. 2018.
[37] A. Zafar, M. Shaqfeh, M.-S. Alouini, and H. Alnuweiri, "Resource allocation for two source-destination pairs sharing a single relay with a buffer," *IEEE Trans. Commun.*, vol. 62, no. 5, pp. 1444–1457, May 2014.
[38] H. Cao, J. Cai, S. Huang, and Y. Lu, "Online adaptive transmission strategy for buffer-aided cooperative NOMA systems," *IEEE Trans. Mobile Comput.*, vol. 18, no. 5, pp. 1133–1144, May 2019, doi: 10.1109/TMC.2018.2854772.
[39] Q. Zhang, Z. Liang, Q. Li, and J. Qin, "Buffer-aided nonorthogonal multiple access relaying systems in Rayleigh fading channels," *IEEE Trans. Commun.*, vol. 65, no. 1, pp. 95–106, Jan. 2017.
[40] S. Luo and K. C. Teh, "Adaptive transmission for cooperative NOMA system with buffer-aided relaying," *IEEE Commun. Lett.*, vol. 21, no. 4, pp. 937–940, Apr. 2017.
[41] M. Shaqfeh, A. Zafar, H. Alnuweiri, and M.-S. Alouini, "Overlay cognitive radios with channel-aware adaptive link selection and buffer-aided relaying," *IEEE Trans. Commun.*, vol. 63, no. 8, pp. 2810–2822, Aug. 2015.
[42] M. J. Neely, "Stochastic network optimization with application to communication and queueing systems," *Synth. Lect. Commun. Netw.*, vol. 3, no. 1, pp. 1–211, 2010.
[43] F. Gao, T. Cui, and A. Nallanathan, "Maximum likelihood channel estimation in decode-and-forward relay networks," in *Proc. IEEE Int. Symp. Inf. Theory*, Jul. 2008, pp. 1233–1237.

Xiaolong Lan received the B.S. degree in mathematics and applied mathematics from the Chengdu University of Technology, China, in 2012. He is currently pursuing the Ph.D. degree with the School of Information Science and Technology, Southwest Jiaotong University, Chengdu, China. From 2017 to 2019, he was a Visiting Ph.D. Student with the University of Victoria. He is also a Visiting Ph.D. Student with Guangzhou University, Guangzhou, China. His current research interests include buffer-aided communication, energy-harvesting wireless communication, and mobile edge computing.

Yongmin Zhang (S'12–M'15) received the Ph.D. degree in control science and engineering from Zhejiang University, Hangzhou, China, in 2015. He was a Visiting Student with the California Institute of Technology, CA, USA, and a Post-Doctoral Research Fellow with the Department of Electrical and Computer Engineering, University of Victoria, BC, Canada. He is currently a Professor with the School of Computer Science, Central South University, Changsha, China. His research interests include resource management and optimization in wireless networks, smart grid, and mobile computing. He received the Best Paper Award from the IEEE PIMRC 2012 and the IEEE Asia-Pacific (AP) Outstanding Paper Award in 2018.

Qingchun Chen (SM'14) received the B.Sc. and M.Sc. degrees (Hons.) from Chongqing University, China, in 1994 and 1997, respectively, and the Ph.D. degree from Southwest Jiaotong University, China, in 2004. He was with Southwest Jiaotong University from 2004 to 2018. He is currently a Full Professor with Guangzhou University, Guangzhou, China. He has authored or coauthored over 100 research articles and two book chapters and holds 40 patents. His research interests include wireless communication, wireless networks, information coding, and signal processing. He received the 2016 IEEE GLOBECOM Best Paper Award. He has been serving as an Associate Editor of the IEEE ACCESS since 2015.

Lin Cai (S'00–M'06–SM'10–F'20) received the M.A.Sc. and Ph.D. degrees (Hons.) in electrical and computer engineering from the University of Waterloo, Waterloo, Canada, in 2002 and 2005, respectively.

Since 2005, she has been with the Department of Electrical and Computer Engineering, University of Victoria, where she is currently a Professor. Her research interests are in the areas of communications and networking, with a focus on network protocol and architecture design supporting multimedia traffic and the Internet of Things. She was a recipient of the NSERC E.W.R. Steacie Memorial Fellowships in 2019, the NSERC Discovery Accelerator Supplement (DAS) Grants in 2010 and 2015, and the Best Paper Awards of the IEEE ICC 2008 and the IEEE WCNC 2011. She has founded and chaired the IEEE Victoria Section Vehicular Technology and Communications Joint Societies Chapter. She has been elected to serve the IEEE Vehicular Technology Society Board of Governors, from 2019 to 2021. She has served as the TPC Symposium Co-Chair for the IEEE Globecom'10 and Globecom'13. She is also a registered Professional Engineer of British Columbia, Canada. She has served as an Area Editor for IEEE TRANSACTIONS ON VEHICULAR TECHNOLOGY, a member of the Steering Committee of IEEE TRANSACTIONS ON BIG DATA (TBD), and IEEE TRANSACTIONS ON CLOUD COMPUTING (TCC), and an Associate Editor for IEEE INTERNET OF THINGS JOURNAL, the IEEE TRANSACTIONS ON WIRELESS COMMUNICATIONS, IEEE TRANSACTIONS ON VEHICULAR TECHNOLOGY, IEEE TRANSACTIONS ON COMMUNICATIONS, *EURASIP Journal on Wireless Communications and Networking*, *International Journal of Sensor Networks*, and *Journal of Communications and Networks* (JCN). She is also a Distinguished Lecturer of the IEEE VTS Society.